POLYMER ENCAPSULATED PARAFFIN WAX TO BE USED AS PHASE CHANGE MATERIAL FOR ENERGY STORAGE

by

MOKGAOTSA JONAS MOCHANE (B.Sc. Hons.)

Submitted in accordance with the requirements for the degree

MASTER OF SCIENCE (M.Sc.)

Department of Chemistry

Faculty of Natural and Agricultural Sciences

at the

UNIVERITY OF THE FREE STATE (QWAQWA CAMPUS)

SUPERVISOR: PROF AS LUYT

9 December 2011

DECLARATION

We, the undersigned, hereby declare that the research in this thesis is Mr Mochane's own original work, which has not partly or fully been submitted to any other University in order to obtain a degree.

_____ _____

Mochane MJ (Mr) Luyt AS (Prof)

DEDICATION

This work is dedicated to my late father (Samuel Mochane), my mother (Elizabeth Mochane) and the entire family of Mochane.

ABSTRACT

The study deals with the preparation and characterization of polystyrene (PS) capsules containing M3 paraffin wax as phase change material for thermal energy storage embedded in a polypropylene (PP) matrix. Blends of PP/PS:wax and PP/PS were prepared without and with SEBS as a modifier. The influence of PS and PS:wax microcapsules on the morphology and thermal, mechanical and conductivity properties of the PP was investigated. The SEM images of the microencapsulated PCM show that the capsules were grouped in irregular spherical agglomerates of size 16-24 μm. However, after melt-blending with PP the much smaller, perfectly spherical microcapsules were well dispersed in the PP matrix. The results also show fairly good interaction between the microcapsules and the matrix, even in the absence of SEBS modification. The FT-IR spectrum of the microcapsules is almost exactly the same as that of polystyrene, which indicates that the microcapsules were mostly intact and that the FTIR only detected the polystyrene shell. The amount of wax in the PS:wax microcapsules was determined as 20-30% from the DSC and TGA curves. An increase in PS:wax content resulted in a decrease in the melting peak temperatures of PP for both the modified and the unmodified blends due to the plasticizing effect of the microcapsules. The thermogravimetric analysis results show that the thermal stability of the blends decreased with an increase in PS:wax microcapsules content as a consequence of lower thermal stability of both the wax and PS. The DMA results show a drop in storage modulus with increasing PS:wax microcapsules content. The microcapsules acted as a plasticizer and thus enhanced the mobility of the polymer chains. Generally the thermal conductivity of the unmodified and modified blends decreased with increasing PS:wax microcapsule content when compared to PP. The polystyrene shell has a lower conductivity than the PP matrix, which explains the lower thermal conductivities of the blends with increasing PS content.

LIST OF ABBREVIATIONS

ABS	Acrylonitrile-styrene-butadiene copolymer
AIBN	2,2'-Azobis(2-methylpropionitrile)
AS	Acrylonitrile-styrene copolymer
BDDA	1,4 butylene glycol diacrylate
C14	n-tetradecane
C15	Carbon 15
C78	Carbon 78
CH_3OH	Methanol
CP	Chemically pure
DBP	Dibenzoyl peroxide
DCP	Dicumyl peroxide
DDM	n-Dodecyl mercaptan
DMA	Dynamic mechanical analysis
DSC	Differential scanning calorimetry
FTIR	Fourier-transform infrared spectroscopy
HD	Hot disk
HDPE	High-density polyethylene
LDPE	Low-density polyethylene
LLDPE	Linear low-density polyethylene
MFI	Melt flow index
MicroPCMs	Microencapsulated phase change materials
MMA	Methyl methacrylate
MPa	Megapascal
N_2	Nitrogen
NaCl	Sodium chloride
O/W	Oil-in-water
PCMs	Phase change materials
PLGA	Poly(lactide-co-glycolide)
PMMA	Poly(methylmethacrylate)
PP	Polypropylene
PS	Polystyrene

SEBS	Polystyrene–block–poly(ethylene-ran-butylene)-block-polystyrene
SEM	Scanning electron microscopy
SLS	Sodium lauryl sulphate
St	Styrene
TEM	Transmission electron microscopy
T_g	Glass transition
TGA	Thermogravimetric analysis
T_m	Melting temperature
$T_{o,m}$	Onset temperature of melting
TPS	Hot disk transient plane source
UV	Ultraviolet light
W/O	Water-in-oil
W_{pp}	Weight fraction of PP
ΔH_m^{cal}	Calculated melting enthalpy
ΔH_m^{obs}	Observed melting enthalpy

TABLE OF CONTENTS

LIST OF TABLES

LIST OF FIGURES

Chapter 1: General introduction

1.1 Background

There are more and more interest in the research of renewable energy sources and materials in the globe with the growing energy crisis [1,2]. There are different forms in which energy can be stored i.e. mechanical, electrical and thermal energy. Amongst the different energy storage forms, thermal energy storage is the most attractive because of the storing and releasing ability [3]. Thermal energy can be stored as a change in internal energy of a material as sensible heat or latent heat, or thermochemical energy storage. Sensible heat storage is carried out by adding energy to the material thus increasing the temperature of the material without changing its phase. Latent heat storage is based upon absorption or release of energy when a storage material undergoes a phase change. Thermochemical energy storage depends on energy absorbed and released by breaking and reforming of molecular bonds in a reversible chemical reaction [3-5].

Amongst the above mentioned thermal energy storage methods, latent heat storage is the most attractive due to high energy storage at a constant temperature corresponding to the phase transition temperature of the storage material [3,9]. The phase change can be solid-liquid, solid-solid, solid-gas or liquid gas. In the solid-solid transition, heat is stored when a storage material is transformed from one crystalline state to another. Generally, this system has small latent heat when compared to solid-liquid transitions. Solid-gas and liquid-gas transitions have high latent heat when compared to solid-liquid transitions, but the major disadvantage is their large volumes which tend to make the system complex and impractical. Solid-liquid transitions are useful because they store a relatively large quantity of heat at a narrow temperature range, with small volume changes [3,6-9].

Phase change materials are latent heat storage materials. The thermal energy transfer occurs when a material changes from solid to liquid or from liquid to solid and this is called a change in phase or state [10]. However, for PCMs to be used as latent heat storage materials these materials must exhibit certain desirable thermal, physical, kinetic, chemical and economical properties (Table 1.1).

Table 1.1 Main desirable properties of PCMs

Thermal properties	Physical properties	Kinetic Properties	Chemical properties	Economical properties
Suitable phase transition temperature	High density	No supercooling	No fire hazard	Abundant
High latent heat of fusion	Small volume change	Sufficient crystallization	No toxicity	Available
Good heat transfer	Low vapour pressure		Long term chemical stability	Inexpensive

To choose a PCM for a certain application, the operating temperature for cooling or heating should match the transition temperature of the PCM. Good heat transfer is required since high conductivity will assist in charging and discharging of energy storage. Phase change materials (PCM) should minimize supercooling since supercooling of a few degrees will interfere with the extraction of energy from the storage material. PCMs should also be non-toxic, non-flammable and non-explosive. Economical PCMs should be available on a large scale and also at a low cost [3,7,11-12].

Phase change materials can be classified into the following categories: Organic compounds, inorganic compounds, and eutectics of inorganic and organic compounds. Inorganic compounds include salt hydrates, salts, metals, and alloys [13,14]. Inorganic PCMs are the most important group of PCMs, especially salt hydrates. The most attractive properties of salt hydrates are: high latent heats, relatively high thermal conductivity, small volume changes on melting, and many salt hydrates are sufficiently available at low cost for their use in energy storage [3,14]. The inorganic materials have not been investigated as extensively as the organic materials because of their undesirable properties such as incongruent melting and supercooling.

The organic materials are classified as non-paraffins and paraffins. The non-paraffins consist of a lot of phase change materials with highly varied properties. Each of these materials will have its own properties. The major properties of these materials include high heat of fusion and inflammability. Their major drawback is their cost, which is 2-2.5 times greater than that of paraffins. They are also mildly corrosive and have low thermal conductivity [3]. Paraffins

are mixtures of many hydrocarbons and have a melting range rather than a sharp melting point. Some of the paraffins investigated for energy storage include waxes, n-eicosane, n-octadecane, and others. Paraffin waxes in particular have been of interest due their promising properties as phase change materials. Paraffin wax is safe, reliable, predictable, less expensive, and non-corrosive. They are chemically inert, show little volume change during melting and have low vapour in the melt [13,15].

Apart from the favourable properties of paraffin waxes, such as congruent melting and self nucleating properties, they are not easy to be used directly in practical applications because of undesirable properties such as leakage, low thermal conductivity and low thermal stability [3,16]. However, all of these undesirable effects can be eliminated by modifying the wax and the storage system [3]. There are different ways in which the storage system can be modified, such as direct incorporation of wax into the polymer and encapsulation of wax by microencapsulation or macroencapsulation. Macroencapsulation is the inclusion of PCM in some form of package such as tubes, pouches, spheres, and panels. Previous experiments with macroencapsulation have failed due to the poor conductivity of the PCM and hence the lack of effective heat transfer [3,11,28]. Microencapsulated or encapsulated PCM is composed of PCM as a core and a polymer shell to maintain the shape and prevent leakage of PCM during a phase change process [19]. The advantages of encapsulated wax are: reduction of the reactivity of the wax with the outside environment, increase in the heat-transfer area, reduction of volume changes as phase change occurs [17-20].

Microcapsules may be obtained by means of chemical or physical methods. The use of some of the techniques has been limited due to high cost of processing, regulatory affairs, and the use of organic solvents, which are of concern for health and the environment. Physical methods include spray drying and fluidized bed processes that are inherently not capable of producing microcapsules smaller than 100 μm. Chemical processes are associated with interfacial, *in situ* and suspension polymerization. Microencapsulation methods based on *in situ* and suspension polymerization techniques were quite successful to produce microcapsules with improved thermal capacity in relation to the PCM content [11,17-18,21].

Even though the PCM is responsible for storage and absorption or release of energy, the selection of an appropriate shell material is important [21,22]. An appropriate shell material is one that withstands hot and dry conditions. Several polymers have been used as PCM shell

materials, and these include gelatine-formaldehyde, toluene-2,4-diisocynate, melamine-formaldehyde, urea-formaldehyde, diethylene triamine and polystyrene [22]. The formaldehyde shell materials such as melamine-formaldehyde, gelatine-formaldehyde and urea formaldehyde have attracted many researchers because of their unique properties such as good seal tightness, endurance, water resistance, alkaline resistance, and fire resistance. However, formaldehyde copolymer shells release the formaldehyde which is poisonous, and this limits their use as shell materials. There is still little information available on the reduction of the formaldehyde content [23]. In the previous studies, PCMs were successfully encapsulated by a single polystyrene (PS) polymer cover [21]. In this context, polystyrene is a promising polymer to be used as shell material in the preparation of microcapsules. In addition, polystyrene has advantages of being hard, clear, easily processed, low cost and a modulus of elasticity between 3200-3600 MPa [22,24].

PCMs absorb and release energy as is shown below in Figure 1.

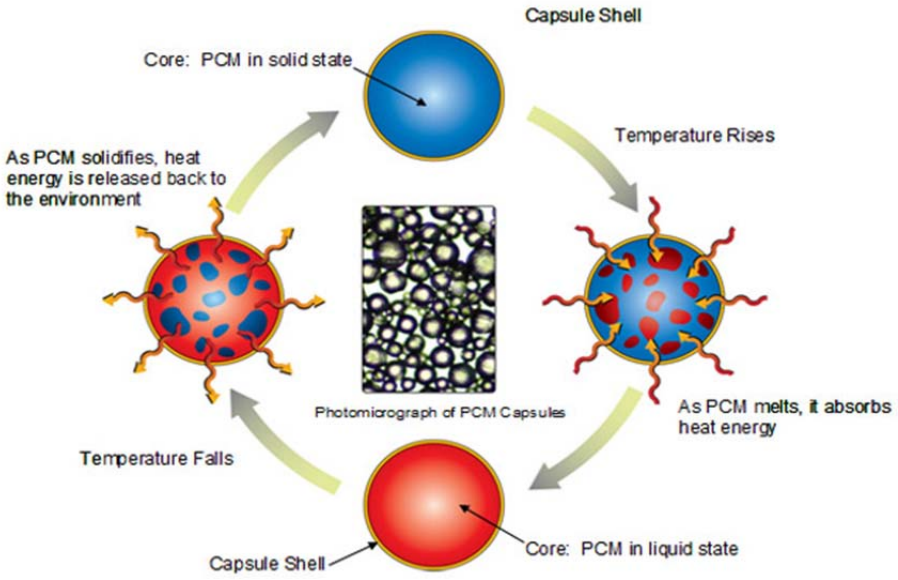

Figure 1 Schematic representation of a phase change process [11]

All materials absorb heat during a heating process while its temperature increases constantly. A large amount of heat is absorbed in the melting process of paraffin waxes inside the polymeric shell. As the surrounding temperature decreases, the PCM inside the polymer starts to crystallize and the PCM capsules release the stored heat energy and consequently the PCM

solidifies. When comparing the heat absorption of phase change materials with those of normal materials, a lot of heat is absorbed by PCMs [11].

In terms of applications, PCM microcapsules can be mixed with gypsum boards to form smart boards. These kinds of smart boards are used as wall materials in buildings, which can absorb solar radiation during the day and release the stored energy during the night. As a result, the room temperature can be maintained in a comfortable range without extra energy which makes the whole system attractive considering energy shortage these days [4,18,25]. To suit for a certain application, PCMs are selected on the basis of their transition temperature [3,27]. For example, materials that melt below 15 °C are used for keeping coolness in air-conditioning applications, while materials that melt above 90 °C are used to drop the temperature if there is sudden increase in temperature [27].

1.2 Objective of the study

The objective of the study was to investigate the morphology and properties of polypropylene (PP) containing PS encapsulated soft paraffin wax. The PS:wax powder (capsules) was mixed into a PP matrix in the composition range of 10-40% and styrene-ethylene/butylene-styrene (SEBS) was used as a compatibilizer to improve the adhesion between the PP and PS. The samples were characterized using scanning electron microscopy (SEM), thermogravimetric analysis (TGA), differential scanning calorimetry (DSC), tensile testing, dynamic mechanical analysis (DMA), Fourier-transform infrared spectroscopy (FTIR), and the hot disk transient plane source (TPS) thermal conductometer.

1.3. Thesis outline

The outline of this thesis is as follows:

- Chapter 1: General introduction
- Chapter 2: Literature review
- Chapter 3: Materials and methods
- Chapter 4: Results and discussion
- Chapter 5: Conclusions

1.4 References

1. C. Cheng, L. Wang, Y. Huang. A novel shape-stabilized PCM: Electrospun ultrafine fibers based on lauric acid/polyethylene terephthalate composite. Materials Letters 2008; 62:3515-3517.
   DOI:10.1016/j.matlet.2008.03.034
2. Q. Cao, P. Liu. Hyperbranched polyurethane as novel solid-solid phase change material for thermal energy storage. European Polymer Journal 2006; 42:2931-2939.
   DOI:10.1016/j.europolymj.2006.07.020
3. A. Sharma, V.V. Tyagi, C.R. Chen, D. Buddhi. Review on thermal energy storage with phase change materials and applications. Renewable and Sustainable Energy Reviews 2009; 13:318-345.
   DOI:10.1016/j.rser.2007.10.005
4. M.M. Farid, A.M. Khudhair, S.A.K. Razack, S. Al-Hallaj. A review on phase change energy storage: Materials and applications. Energy Conversion and Management 2004; 45:1597-1615.
   DOI:10.1016/j.enconman.2003.09.015
5. S.M. Hasnain. Review on sustainable thermal energy storage technologies, Part 1: Heat storage materials and techniques. Energy Conversation and Management 1998 ;39:1127-1138.
   DOI:10.1016/SO196-8904(98)00025-9
6. I. Krupa, G. Miková, A.S. Luyt. Polypropylene as a potential matrix for the creation of shape stabilized phase change materials. European Polymer Journal 2007; 43: 895-907.
   DOI:10.1016/j.eurpolymj.2006.12.019
7. A.F. Regin, S.C. Solanki, J.S. Saini. Heat transfer characteristics of the storage system using PCM capsules: A review. Renewable and Sustainable Energy Reviews 2008; 12: 2438-2458.
   DOI:10.1016/j.rser.2007.06.009
8. H.S. Fath. Technical assessment of solar thermal energy storage technologies. Renewable Energy 1998; 14: 35-40.
   DOI:10.016/SO960-1481(98)00044-5

9. C. Alkan, A. Sari. Fatty acid/poly(methyl methacrylate) (PMMA) blends as form-stable phase change materials for latent heat thermal energy storage. Solar Energy 2008; 82: 118-124.
DOI:10.1016/j.solener.2007.07.001

10. A.S. Luyt, I. Krupa. Phase change materials formed by UV curable epoxy matrix and Fischer-Tropsch paraffin wax. Energy Conversion and Management 2009; 50:57-61.
DOI:10.1016/j.enconman.2008.08.026

11. S. Mondal. Phase change materials for smart textiles – An overview. Applied Thermal Engineering 2008; 28:1536-1550.
DOI:10.1016/j.applthermaleng.2007.08.009

12. B.C. Shin, S.D. Kim, W.H. Park. Phase separation and supercooling of a latent heat-storage material. Energy 1989; 14:921-930.
DOI:10.1016/0360-5442(89)90047-9

13. J.A. Molefi, A.S. Luyt, I. Krupa. Comparison of LDPE, LLDPE and HDPE as matrices for phase change materials based on a soft Fischer-Tropsch paraffin wax. Thermochimica Acta 2010; 500:88-92.
DOI:10.1016/j.tca.2010.01.002

14. M.M. Farid, A.M. Khudhair, S.A.K. Razack, S. Al-Hallaj. A review on phase change storage: Materials and applications. Energy Conversion and Management 2004;45:1597-1615.
DOI:10.1016/j.enconman.2003.09.015

15. Z. Jin, Y. Wang, J. Liu, Z. Yang. Synthesis and properties of paraffin capsules as phase change materials. Polymer 2008; 49:2903-2910.
DOI:10.1016/j.polymer.2008.04.030

16. G. Fang, H. Li, F. Yang, X. Liu, S. Wu. Preparation and characterization of nano-encapsulated n-tetradecane as phase change material for thermal energy storage. Chemical Engineering Journal 2009; 153:217-221.
DOI:10.1016/j.cej.2009.06.019

17 C. Liang, X. Lingling, S. Hongbo, Z. Zhibin. Microencapsulation of butyl stearate as a phase change material by interfacial polycondensation in a polyurea system. Energy Conversion and management 2009; 50:723-729.
DOI:10.1016/j.enconman.2008.09.044

18. X.L. Shan, J.P. Wang, X.X. Zhang, X.C. Wang. Formaldehyde-free and thermal resistant microcapsules containing n-octadecane. Thermochimica Acta 2009; 494:104-109.
DOI:10.1016/j.tca.2009.04.026

19. G. Fang, Z. Chen, H. Li. Synthesis and properties of microencapsulated paraffin composites with SiO_2 shell as thermal energy storage materials. Chemical Engineering Journal 2010; 163:154-159.
DOI:10.1016/j.cej.2010.07.054

20. M.N.A. Hawlader, M.S. Uddin, M.M. Khin. Microencapsulated PCM thermal-energy storage system. Applied Energy 2003; 74:195-202.
DOI:10.1016/SO306-2619(02)00146-0

21. L. Sánchez, P. Sánchez, A. de Lucas, M. Carmona, J.F. Rodriguez. Microencapsulation of PCMs with a polystyrene shell. Colloid and Polymer Science 2007; 285:1377-1385.
DOI:10.1007/s00396-007-1696-7

22. L. Sánchez-Silva, J.F. Rodriguez, A. Romero, A.M. Borreguero, M. Carmona, P. Sánchez. Microencapsulation of PCMs with styrene-methyl methacrylate copolymer shell by suspension-like polymerization. Chemical Engineering Journal 2010; 157:216-222.
DOI:10.1016/j.cej.2009.12.013

23. L. Wei, Z.X. Xiang, W.X. Chen, N.J. Jin. Preparation and characterization of microencapsulated phase change material with low remnant formaldehyde content. Materials Chemistry and Physics 2007; 106:437-442.
DOI:10.1016/j.matchemphys.2007.06.030

24. S.A. Samsudin, A. Hassan, M. Mokhtar, S.M.S. Jamaluddin. Chemical resistance evaluation of polystyrene/polypropylene blends: Effect of blend compositions and SEBS content. Malaysian Polymer Journal 2006; 1:11-24.

25. R. Yang, Y. Zhang, X. Wang, Y. Zhang, Q. Zhang. Preparation of n-tetradecane-containing microcapsules with different shell materials by phase separation method. Solar Energy Materials and Solar Cells 2009; 93:1817-1822.
DOI:10.1016/j.solmat.2009.06.019

26. Y. Cai, L. Song, Q. He, D. Yang, Y. Hu. Preparation, thermal and flammability properties of a novel form-stable phase change materials based on high density polyethylene/poly(ethylene-co-vinylacetate)/organophilic montmorilonite nanocomposites/paraffin compounds. Energy Conversion and Management 2008; 49:2055-2062.
DOI:10.1016/j.enconman.2008.02.013

27. G. Fang, H. Li, F. Yang, X. Liu, S. Wu. Preparation and characterization of nano-encapsulated n-tetradecane as phase material for thermal energy storage. Chemical Engineering Journal 2009; 153:217-221.
DOI:10.1016/j.cej.2009.06.019

28. A. Pasupathy, R. Velraj, R.V. Seeniraj. Phase change material-based building architecture for thermal management in residential and commercial establishments. Renewable and Sustainable Energy Reviews. 2008;12:39-64.
DOI:10.1016/j.rser.2006.05.010

Chapter 2: Literature review

2.1 Introduction

2.1.1 Definition of paraffin wax, sources, and uses

Paraffin wax is a tasteless and odourless white translucent solid hydrocarbon. The source of paraffin wax is petroleum. Typically, waxes are produced as extracted residues during the dewaxing of lubricant oil. It consists of mixture of solid aliphatic hydrocarbons of high molecular weight having the general formula C_nH_{2n+2}. Paraffin wax is used in the manufacture of candles, paper coating, protective sealant for food products and beverages, glass-cleaning preparations, floor polishing and stoppers for acid bottles [1-3]. The specific heat capacity of latent heat paraffin waxes is about 2.1 J g^{-1} K^{-1} and their melting enthalpy lies between 180 and 230 J g^{-1}. The combination of these two values results in an excellent energy storage density [4-5].

Hydrocarbons with more than 17 carbon atoms per molecule are waxy solids at room temperature. The molecular weight, melting temperature and heats of fusion of paraffin waxes increase with an increase in the number of carbon atoms. The carbon atom chain lengths for paraffin waxes with a melting temperature range between 30 and 90 ˚C range from 18 to 50 (C18-C50), and the viscosity of paraffin wax increases with increasing molecular weight. Because of steric effects caused by the arrangements of atoms in the molecule, there is a difference between hydrocarbons (paraffin wax) with odd and even number of carbon atoms. The even numbered hydrocarbons have higher latent heat of fusion than the odd numbered ones, as illustrated by Table 2.1 [6].

Table 2.1 Technical data for n-alkanes

n-Alkanes	Number of carbons	Molecular weight (g mol^{-1})	Melting point (K)	Latent heat (J g^{-1})
Heptane	7	100	182.6	141
Octane	8	114	216.4	181
Nonane	9	128	219.7	170
Decane	10	142	243.5	202
Undecane	11	156	247.6	177
Dodecane	12	170	263.6	216
Tridecane	13	184	267.8	196
Tetradecane	14	198	278.9	227
Pentadecane	15	212	283.1	207
Hexadecane	16	226	291.3	236
Heptadecane	17	240	295.1	214
Octadecane	18	254	301.3	244
Nonadecane	19	268	305.2	222
Eicosane	20	282	309.8	248
Heneicosane	21	296	313.4	213
Docosane	22	310	317.2	252
Tricosane	23	324	320.7	234
Tetracosane	24	338	338.0	255
Pentacosane	25	352	323.8	238
Hexacosane	26	366	326.7	250
Heptacosane	27	380	329.5	235
Octacosane	28	394	331.9	254
Nonacosane	29	408	336.4	239
Triacontane	30	422	338.6	252

2.2 Preparation and morphology

2.2.1 Polymer/wax blends

Paraffin waxes blended with polymers appear to be the best candidates for the preparation of smart polymeric phase change materials for different applications. A polymeric matrix fixes the phase change material in a compact form and suppresses leaking. A variety of polymer matrices, based on thermoplastic and thermoset resins, are available with a large range of chemical and mechanical properties. Polyethylene seems to be most frequently used polymer for blending with paraffin waxes to obtain PCMs. Polyolefin/wax blends were mainly prepared by melt extrusion, melt mixing and mechanical methods [1-5,7-13]. Each of these mixing methods results in different properties of the blends. To investigate the morphology of polyolefin/wax blends, techniques such as scanning electron microscopy (SEM), differential scanning calorimetry (DSC), and transmission electron microscopy (TEM) were used. Most studies have demonstrated that at 30% wax content and more a two- phase morphology is observed which implies the immiscibility of the polyolefins and wax [7,14]. SEM images of the polyolefin/paraffin wax blends indicate that paraffin wax disperses in the three-dimensional net structure formed by polymers [11,13]. Luyt and co-workers [4] indicated that the miscibility and behaviour of polyolefin/wax blends do not only depend on the structure and molecular weight of waxes, but also on the structures of the polymers.

Several thermoplastic polymers have been blended with different grades of paraffin wax to form polyolefin/wax blends. Polyethylenes and polypropylene belong to the most studied matrices [1-14]. Krupa et al. [4] investigated phase change materials based on low-density polyethylene blended with respectively soft and hard paraffin waxes. The blends were prepared by melt mixing. The SEM images showed differences in morphology for the two types of blends. LDPE blended with a hard Fischer-Tropsch paraffin wax showed a homogenous surface with slight wax separation, whereas the same polymer blended with a soft paraffin wax showed immiscibility between the two phases. The reason for the different morphologies was the difference in morphology of the two waxes, i.e. the soft paraffin wax had a low molecular weight and was able to separate from the blends much easier than the hard wax, with its higher molecular weight.

Krupa *et al.* [5] investigated polypropylene as a potential matrix for the creation of shape stabilized phase change materials. The same types of waxes mentioned in the previous paragraph were blended with polypropylene by melt mixing to form polyolefin/wax blends. In this case, however, the SEM images showed immiscibility of both types of waxes with polypropylene. The thermal and mechanical properties of extruded LLDPE/wax blends were also investigated [1]. The SEM pictures showed that an increase in wax content causes LLDPE/wax blends to rupture along different lines, and the immiscibility at wax contents greater than 20% was confirmed by DSC.

High density polyethylene was blended with paraffin wax to form shape-stabilized composites [11]. Different types of paraffin wax (refined and semi-refined) were used during blending. The preparation of the blends was done through melt mixing. It was observed from the SEM micrographs that both semi-refined and refined paraffin wax had similar textures. It was further observed that the paraffin wax was contained in the three-dimensional netted structure of the solidified HDPE. Similar SEM micrographs were observed when HDPE was blended with a paraffin hybrid through melt extrusion [13].

2.2.2 Microencapsulated phase change materials (MicroPCMs)

Several researchers prepared microcapsules with different shell/core ratios in order to find the optimum conditions to prepare stable microcapsules with the greatest phase change enthalpy [15-19]. Several physical and chemical methods have been developed for the production of microcapsules. The most often used microencapsulation methods are polymerization methods such as *in situ,* suspension, and interfacial polymerization. In these polymerization methods the monomers polymerise around droplets of an emulsion and form a solid polymeric wall. There are certain parameters that have a significant influence on the size and shape of the capsules. Most studies found that parameters such as shell/core ratio, chain transfer agent, types of monomers, effect of stirring rate, and addition of modifiers were important when preparing the capsules [19-28]. These researchers also found four types of morphologies depending on these factors [19-33]. The observed morphologies were: well-encapsulated capsules, half moon capsules, irregular capsules and pure polymer (no core) particles. These findings demonstrated that when the content of the core (paraffin wax) was higher than that of the polymer, the shell material became rather thin and fragile. The SEM pictures of the microcapsules showed shells with semi-spherical or irregular shapes. The authors concluded

that the polymer formed a very thin film so that the polymer shell could be broken because of volume shrinkage of the paraffin wax. The studies also demonstrated that well-encapsulated microcapsules were found with a higher ratio of polymer (shell) to paraffin wax or with a 1:1 ratio of the two materials.

Fang *et al.* [19] prepared nanoencapsulated phase change material using a higher polymer to paraffin wax content. The nanocapsules with polystyrene as the shell material and n-octadecane as the core were synthesized by miniemulsion *in situ* polymerization. SEM photos showed regular spheres, because of the addition of chain transfer agent which decreases the molecular weight of the formed polymer chains and increase the mobility of the polymer. In view of the kinetics of phase separation, the authors suggested that a network polymer might hinder the formation of capsules. The use of higher molecular weight polymer results in poor mobility of the polymer, giving rise to irregular spheres because the time was not enough to spread and form a smooth surface. The study also showed that over-addition of a chain transfer agent results in higher mobility and a loss of polymer strength. Microcapsules with butyl stearate as a phase change material were prepared by interfacial polycondensation in a polyurea system [20]. The appropriate ratio by weight of core and shell of microencapsulated PCMs was 4:1. Optical microphotographs of the microencapsulated PCMs showed that the surface of the capsules was smooth and the shape was very regular. There was no explanation given by the authors about the polymer strength in the system.

Rui *et al.* [26] investigated n-tetradecane-containing microcapsules with different shell materials prepared by a phase separation method. Three shell materials were used to encapsulate n-tetradecane (C14), i.e. acrylonitrile-styrene-copolymer (AS), acrylonitrile-styrene-butadiene copolymer (ABS) and polycarbonate (PC). The morphologies of the microcapsules were studied by SEM. Only PC/C14 microcapsules were regularly spherical, while the microcapsules with ABS/C14 and AS/C14 were irregular and semi-spherical. The authors suggested that the difference was most likely due to dynamic factors, including viscosity of the solution, evaporation rate of the solvent, and the mobility of the shell material.

Fan *et al.* [15] investigated super-cooling prevention of microencapsulated phase change material using a melamine-formaldehyde resin shell. The microcapsules were prepared by *in situ* polymerization. The effects of the nucleating agents, including sodium chloride, 1-

octadecanol, and paraffin were studied. The findings of the study showed that all nucleating agents prevented supercooling, but the surfaces of sodium chloride and 1-octadecanol were rough and the microcapsules were agglomerated. Similar SEM results were obtained for the preparation of nano-encapsulated n-tetradecane as a phase change material using urea and formaldehyde as shell materials [31]. The nanocapsules were prepared by *in situ* polymerization and resorcin was used as a modifier. The authors observed a roughness of the capsules at high concentrations of resorcin, which causes an increases in the stickiness of the capsule and makes them hard to form regular spheres. Similar appearance was observed in the preparation of microcapsules using a styrene-methyl methacrylate copolymer as shell material by suspension like polymerization [17]. An MMA/St mass ratio of 4.0 and a monomer/paraffin ratio of 3.0 were used in the preparation of these microcapsules.

Zhang *et al.* [30] investigated the properties of microcapsules and nanocapsules containing n-octadecane. The capsules were prepared by emulsion polymerization at a shell/core ratio of 1:1. The effects of stirring rate and contents of emulsifier were investigated in this study. The stirring rate and emulsifier had effects on the morphology of the microencapsulated n-octadecane. The surfaces of the microcapsules became smoother when the stirring rate and content of the emulsifier increased in the microcapsules.

2.3 Thermal properties

2.3.1 Polymer/paraffin wax blends

A lot of work has been done on the thermal properties of polymer/wax blends. In the past Luyt and co-workers investigated the influence of blending with different types of waxes, as well as cross-linking, on the thermal properties of polyolefins, especially polyethylenes and polypropylene. The blends were prepared by mechanical mixing, melt mixing and melt extrusion. Each of these methods resulted in different properties of the blends. Generally, the studies demonstrated that the melting enthalpies of the blends increased with an increase in wax content [1-5,7-10]. Thermal properties such as melting points (T_m), onset temperatures of melting ($T_{o,m,}$), and melting enthalpies (ΔH) were strongly affected by the use of cross-linking agents [2,10]. Dicumyl peroxide (DCP) and dibenzoyl peroxide (DBP) were used as cross-linking agents in these studies. Generally there was a decrease in melting temperatures

and enthalpies with an increase in content of both cross-linking agents. The authors suggested that the presence of cross-linking agents reduces the polyethylene (in this case LLDPE and LDPE) and wax crystallinities.

Krupa and Luyt studied the thermal properties of isotactic polypropylene/hard Fischer-Tropsch paraffin wax blends [7]. The DSC results indicated that polypropylene (PP) and hard paraffin wax were homogenous on a macro-scale when the wax content is less than 10%, whereas, at higher wax concentrations, there is a clear separation between the wax and PP melting endotherms. The thermal and mechanical properties of extruded LLDPE/wax blends were also investigated [1]. In this case the results were different from the previous study because the DSC measurements indicated that blends consisting of 10% and 20% of wax were probably miscible in the crystalline phase. However, for 30% and more wax, phase separation of the two components was observed.

Mpanza and Luyt studied the influence of three different waxes (EnHance wax, H1 and M3 wax) on the thermal and mechanical properties of low-density polyethylene (LDPE) [9]. The authors found that the DSC curves of LDPE mixed with EnHance (1, 3, 5 and 10 wt %) showed one endothermic peak for all the blends. The enthalpy was found to increase with increasing wax content. The DSC curves for LDPE and H1 wax showed that they were miscible up to 3 wt% wax content. It was also observed that the melting enthalpy of the blends increase with increase in H1 content, but that the crystallinity was lower than that of LDPE/EnHance. The reason given was that EnHance had a high crystallinity than H1 wax. LDPE/M3 wax blends showed miscibility up to 5 wt% wax and the melting enthalpies decreased with increasing wax content. The authors concluded that M3 wax probably crystallized in the amorphous phase of LDPE because of the shorter chains of the M3 wax.

The same matrix (LDPE) was blended with soft and hard paraffin waxes respectively [4]. The DSC results showed that the hard paraffin wax was more miscible with LDPE because of co-crystallization than the soft paraffin wax. The melting enthalpies of both types of blends increased with an increase in wax content because of the higher wax crystallinity. In all cases the blends were prepared by melt mixing.

Most of the investigated polyethylene/wax blends were miscible at 10 and 20 wt % wax contents, and the melting enthalpies increased with increase in wax content in most cases.

However, blending of paraffin waxes with polypropylene showed miscibility only at wax contents less than 10 wt %. The melting enthalpies increased with an increase in wax content [5-7,9]. Luyt and Krupa investigated polypropylene as a potential matrix for the creation of shape stabilized phase change materials [5]. The blends consisting of hard and soft paraffin wax were prepared by melt mixing. The findings of the study demonstrated that both grades of paraffin wax were not miscible with PP due to different crystalline structures. However, it was shown that the hard Fischer-Tropsch paraffin wax was more compatible with PP than the soft paraffin wax.

2.3.2 Microencapsulated phase change materials (MicroPCMs)

PCMs require high latent heat storage capacity in thermal energy storage applications. In terms of nano-encapsulated and microencapsulated materials, only the core materials absorb/release thermal energy during the heating/cooling process. It is clear that a high core material content will result in a high latent heat storage capacity [21]. A lot of effort has been devoted to the determination of the thermal properties of microencapsulated phase change materials [24-30,34]. Most researchers reported thermal properties such as latent heat, subcooling degree, melting temperature, and viscosity as the most important ones in energy storage applications [17,24-30,34]. Subcooling was reported by most researchers as a serious problem in PCM research and applications [17,34-37]. It was reported in these studies that subcooling drastically deteriorates the system performance and reduce energy efficiency.

There are several kinds of materials that can be used as nucleating agents to suppress subcooling of MicroPCMs [15,34,38]. Alvarado *et al*. [38] experimentally characterized the thermal behaviour of bulk and microencapsulated n-tetradecane by using DSC. The subcooling degree was specifically studied and silica fume was employed as a nucleating agent. The findings of the study indicate that silica fume could only suppress the subcooling of the bulk material, while 0.2 wt% of silica fume was not effective for MicroPCMs. A comparative study by using a more stable nucleating agent, 1-4 wt% tetradecanol, showed that 2 wt% of tetradecanol was already effective in suppressing subcooling.

There are other materials that can also be used as nucleating agents. Fan *et al*. [15] prepared three kinds of MicroPCMs (n-octadecane as the core material) with sodium chloride, 1-octadecanol and paraffin respectively as the nucleating agents. They found that the

subcooling could be effectively suppressed by increasing the concentration of the nucleating agent to 6, 9 and 20 wt% respectively for sodium chloride, 1-octadecanol and paraffin. The target of most researchers was to prepare microcapsules with a phase change enthalpy as large as possible [22,26,28,34-37]. Most of them to confirm if the paraffin wax has been encapsulated, or if the microcapsules were only constituted of polymer. In order to do this, they analysed microPCMs by means of differential scanning calorimetry (DSC). Sánchez *et al.* [35] prepared microcapsules of PCMs with a polystyrene shell. The mass ratio of the paraffin to polymer was maintained at 27:78. The study showed that the latent heat of the microcapsules, which was of 41.7 J g^{-1}, was smaller than that of pure paraffin wax. The authors suggested that this value indicated that not all the paraffin of the initial recipe had been encapsulated, as expected from the fact that a thin layer of paraffin had been obtained at the end of the experiment. Similar results were obtained by several other researchers [15-18,24-29,34,36-38]. These authors demonstrated that in order to minimize the loss of paraffin wax after polymerization, a series of experiments using different core to coating ratios have to be performed to find the best encapsulation ratio.

The phase change properties of microcapsules can be affected by other factors such as the stirring rate, the core/shell ratio and the content of the emulsifier [18,25,27-28,35,38-39]. All these factors are very important for the application of microencapsulated or nanoencapsulated PCMs in fabrics and fibres. Zhang *et al.* [39] investigated the fabrication and properties of microcapsules and nanocapsules containing n-octadecane. The effects of stirring rate and contents of emulsifier on the phase change properties were studied using DSC. The findings of the study indicated that the stirring rate had no effect on the crystal content of n-octadecane encapsulated in the microcapsules. However, the melting enthalpies decreased gradually with an increase in emulsifier content. The authors suggested that such a trend shows that the emulsifier was encapsulated in the microcapsules. However, in another study by the same group [40] it was observed that the stirring rate did have an effect on the melting enthalpies of the microcapsules. In this study, the melting enthalpies decreased with increasing stirring rate. Surprisingly the authors made no comment on the fact that they observed different trends on comparable systems.

Sánchez *et al.* [41] studied the influence of operation conditions on the microencapsulation of PCMs. The findings of the study demonstrated that the stirring rate and the core/shell ratio had an influence on the phase change properties of microencapsulated PCMs, unlike the

results obtained by Zhang *et al*. [39]. The results showed that with an increase in stirring rate the particle size decreased and the melting enthalpy increased. The main reason for the decrease in particle size is that the stirring rate affects both the formation of drops and the aggregation through collisions between neighbouring globules. Obviously, under vigorous stirring, when the aggregations of globules are minimized, smaller particles are obtained. The authors in this study observed that the smallest particles showed the largest amount of encapsulated PCM (the high melting enthalpies).

Several researchers showed that the energy capacity depends on the core-to-coating ratio [28,35,40-41]. The study of Sánchez *et al*. [41] in terms of the core/shell ratio showed that using different core to coating ratios in the range from 0.35 to 2.00, the paraffin/styrene mass ratio 0.50 encapsulated more paraffin wax and hence had a higher melting enthalpy. The same system of paraffin/styrene was studied using four different paraffin waxes [35]. The authors found that the best mass ratio of core/coating was 27:78. The authors suggested that if the amount of monomers was not enough, the core materials were not completely encapsulated; in other words, as the relative amount of PCM increases in the recipe, it was more difficult to encapsulate by the polymer. A similar observation was made by Fang *et al*. [37] in the preparation of nanoencapsulated phase change materials. The authors observed that when the core/shell ratio was 3:2, the polymer became thin and fragile with a loss of core material and hence a decrease in melting enthalpy. However, with a core/shell ratio of 1:2, energy was stored because the polymer could withstand volume shrinkage during the core crystallization.

A number of researchers prepared microcapsules with 1:1 core/shell ratios or with high core content compared to the polymer, and still more energy was stored [18-21,28-29,42]. In most studies the phase change temperature of the microencapsulated PCM was very close to that of the core, suggesting that the thermal properties of the MiroPCMs were similar to that of the core material [15-18,21-25,27-30,35-37,43-46]. However, Alay *et al*. [42] prepared microcapsules with 50/50 ratio of core/shell using PMMA as a shell and hexadecane as core material. Two types of cross-linker, namely allyl methacrylate and ethylene glycol dimethacrylate were used. They found that the two cross-linkers had a significant influence on the phase change temperatures and the melting enthalpies. The melting temperature of the core material (hexadecane) decreased to lower temperatures in the presence of both cross-

linkers. The melting enthalpy of the microcapsules with ethylene glycol dimethacrylate were higher than that of the microcapsules with allyl methacrylate.

Similar results were obtained by a number of researchers without the use of cross-linkers [19,21,29]. The phase change temperature of the microencapsulated PCM was very close to that of the bulk material (core) in the absence of cross-linkers. However, the role of the cross-linking agent is important for the hardening of the coating materials. A number of researchers have also prepared microcapsules or nanocapsules with higher core contents [18,20,24,28]. Very high energy storage and release capacities were found for all the capsules prepared. Although higher values of core-to-coating ratio increased the heat capacity, the strength of the polymer at higher core content was not discussed in these papers.

2.4 Thermal stability

2.4.1 Polymer/wax blends

There are a few studies on the preparation and investigation of the thermal stabilities of polymer/wax blends [1-5,14]. The thermal stability of polyolefin/wax blends showed large dependence on wax content in the blend systems. Various authors [2-3,7-8,10] demonstrated that an increase in wax mass fraction in the blends led to a decrease in the thermal stability of the blends. It did not matter which kind of wax or polymer matrix was used in the system. The authors attributed this behaviour to the low thermal stability of waxes compared to that of the polymer matrices. The studies also demonstrated that in most cases the blends were more thermally stable than the pure waxes due the presence of the thermally more stable polymer matrices.

However, some authors obtained different results on the thermal stability at low wax contents, specifically using low-density polyethylene as a matrix. Luyt and Mpanza [9] studied the comparison of different waxes as processing agents for low-density polyethylene (LDPE) using three different waxes (i.e. M3, EnHance and H1) at low contents. In this case not all the polymer/wax blends were thermally less stable than the pure LDPE. The authors found that a small amount of wax improved the thermal stability of the polymer. The samples containing 1% wax for all the investigated blends were the most stable, and the stability decreased with increasing wax content. Up to 10% wax, which was the highest wax content

used in this study, the thermal stability of the blends did not fall below that of the pure LDPE. According to the authors the addition of wax improved the crystallinity of the polymer and as a result its thermal stability. However, because of the lower thermal stability of the wax itself, the thermal stability did not increase with increasing wax content.

Luyt and Krupa [26] investigated phase change materials formed by a UV curable epoxy matrix and a Fischer-Tropsch paraffin wax. The authors demonstrated some interesting observations regarding the thermal stability of the blends. It was found that the mixtures decomposed in only one distinguishable step, whereas immiscible blends usually degrade in two steps. The authors suggested that the epoxy resin may have acted as a heat isolator so that it took longer for the heat energy to reach the wax particles, which resulted in the wax starting to decompose at higher temperatures. The results were in line with the studies carried out by Luyt and co-workers using the same wax (hard Fisher-Tropsch paraffin wax) but in this study it was also compared with a soft wax in PP and LDPE as matrices [4-5]. In both cases the blends with the soft wax degraded in two distinguishable steps, while those with the hard wax degraded in only one step. The results indicated a higher level of compatibility of the hard paraffin wax with both PP and LDPE compared to the soft wax. The results also showed that the blends containing the hard wax had a significantly higher thermal stability than those containing the soft wax at the same wax content.

2.4.2 Microencapsulated phase change materials (MicroPCMs)

The key to successful microencapsulation is to design a microcapsule that is well suited for the intended application [47]. In selecting a polymer for the microcapsule wall, thermal stability is important, and the wall forming polymer should be sufficiently stable during storage and application [48]. Thermal stability of microcapsules is an important property to facilitate production, handling and application. As the stability of the capsules increases, their durability will also increase and the leakage possibility of the material will decrease [49]. The thermal stability is normally determined by a thermogravimetric analyzer (TGA). The thermal stability of MicroPCMs has been studied by a number of researchers [19,21,27,29,35,37,42,50]. The findings of the studies demonstrated that microcapsules normally degrade in two steps. The first degradation step at lower temperatures normally belongs to the paraffin waxes, while the second degradation step at higher temperature belongs to the polymers, depending on the type of polymer used.

There are certain factors that have a significant effect on the thermal stability of microcapsules. For an example, the mechanisms of weight loss in air and in nitrogen are different. It was demonstrated that the weight loss of pure paraffin wax (hexadecane in this case) was 120 °C in air and nitrogen. However, the degradation temperature of microencapsulated hexadecane in N_2 and air was determined to be 330 and 255 ˚C respectively. The thermal stability of microencapsulated PCMs can be improved by additives such as sodium chloride (NaCl) introduced during polymerization. Fang *et al*. [16] used n-tetradecane as the core material and urea-formaldehyde as the shell material, and sodium chloride as an additive. The capsules produced from oil/water emulsion containing 1-3% NaCl stabilized the urea-formaldehyde prepolymer and improved encapsulation. However, greater weight losses were observed at a higher additive concentrations (8 and 10%). The authors suggested that at higher NaCl concentrations the additive inhibited the reaction of the prepolymer and hence the stability decreased.

Thermal stability was also improved with the addition of cross-linkers such as 1,4 butylene glycol diacrylate (BDDA), allyl methacrylate and ethylene glycol dimethacrylate [27,42]. It was found that the higher the cross-linking agent content, the higher the thermal resistance temperatures of the MicroPCMs. The formation of cross-linked polymer strengthened the shell material. Shan *et al*. [27] showed that the core/shell mass ratios had a significant effect on the thermal stability of MicroPCMs. They demonstrated that as the content of the shell increased, the thickness of the shells of all the microcapsules increased. Therefore the core could not easily diffuse out from the microcapsule.

2.5 Chemical structure

Of the two systems employed for thermal energy storage i.e. polymer/wax blends and MicroPCMs, a lot of work has been done on the chemical structure analysis of MicroPCMs using FT-IR spectroscopy [15-18,21-25,27-29,35-36]. Generally, FT-IR spectroscopy was used to characterize the microcapsules structurally because it was possible to prove the existence of materials in the microcapsules by FT-IR spectroscopy. Most studies proved the co-presence of polymers and paraffin waxes in the microcapsules [15-18,21-25,27-29,35-37]. The studies showed that the absorption peaks of the paraffin wax did not change in the MicroPCMs spectra. The results indicated that there were no chemical interaction between

the paraffin molecules and the polymers. It was suggested that the paraffin was easily encapsulated in the polymer shells through the different polymerization methods. Factors such as core/shell ratio and stirring rate did not seem to significantly change the FT-IR spectra of the microcapsules [30].

Fang *et al*. [36] prepared microencapsulated paraffin composites with an SiO_2 shell as thermal energy storage materials. FT-IR spectroscopy was used to prove the co-presence of the paraffin and the SiO_2 in the microcapsules. The absorption peaks of both the SiO_2 and the paraffin wax appeared in these spectra. Sánchez *et al*. [17] prepared microencapsulated PCMs with a styrene-methyl methacrylate copolymer shell by suspension polymerization. The chemical composition of the capsules was characterised by FT-IR. The relative proportions of St/MMA in the microcapsules were determined by taking into account the peak intensity ratio of the characteristic peaks of PMMA (1735 cm^{-1}) and PSt (735 cm^{-1}). The authors observed a decrease in the ratio of the peak intensities as the St content decreased. Alay *et al*. [42] synthesized microcapsules of PMMA/hexadecane using different cross-linkers. FT-IR spectroscopy was used to structurally characterize the microcapsules. The study revealed slight differences in the FT-IR spectra of the microencapsulated particles due to the differences in cross-linkers used. However, the differences between the peaks were not significant because the use of cross-linker in the synthesis was maximum 2 %.

2.6 Mechanical properties

2.6.1 Polymer/wax blends

The mechanical properties of polyolefin/wax blends were mainly reported by Luyt and co-workers [1,3,6,9-10,52]. In these studies it was generally found that the Young's moduli of the blends were dependent on the wax content, and normally increased with an increase in wax content in the blends. This was associated with the high degree of crystallinity of the waxes compared to the different polyolefin matrices. However, the modulus of HDPE/wax blends decreased with increasing wax content [52]. This was associated with the fact that wax had a lower crystallinity than HDPE.

Elongation at yield and yield stress did not show similar trends, but varied according to the polymer/wax system investigated. A few studies showed shown that the yield stress increased

with increasing wax content in the blends [1,9]. This behaviour was expected, since wax increases the crystallinity of the blend, and yield stress depends on crystallinity. Some studies [1,6] reported a reduction in elongation at yield with an increase in wax content. This was attributed to the crystallization of wax in the amorphous part of the polymer, restricting the polymer chain mobility. However, other authors found that wax content had no influence on the yield point (elongation at yield and yield stress) [3].

Some studies showed that stress and elongation at break depends on the wax concentration [1,9,52]. Generally the elongation at break of the polyolefins decreased with increasing wax content. The main reason given was that the wax molecules were too short to form tie chains, and that the number of dislocations increased with an increase in wax content. This decreased the strain at break. The stress at break generally decreased with increasing wax content. The authors suggested that the wax crystallized in the amorphous part of the polymer, forming stress concentration points, or reduced the number of tie chains when co-crystallizing with the polymer.

2.7 References

1. I. Krupa, A.S. Luyt. Thermal and mechanical properties of extruded LLDPE/wax blends. Polymer Degradation and Stability 2001; 73:157-161. DOI:10.1016/S0141-3910(01)00082-9
2. I. Krupa, A.S. Luyt. Thermal properties of uncross-linked and cross-linked LLDPE/wax blends. Polymer Degradation and Stability 2000; 70:111-117. DOI:10.1016/S0141-3910(00)00097-5
3. I. Krupa, A.S. Luyt. Physical properties of blends of LLDPE and an oxidized paraffin wax. Polymer 2001; 42:7285-7289. DOI:10.1016/S0032-3861(01)00172-0
4. I. Krupa, G. Miková, A.S. Luyt. Phase change materials based on low-density polyethylene/paraffin wax blends. European Polymer Journal 2007; 43:4695-4705. DOI:10.1016/j.eurpolymj.2007.08.022
5. I. Krupa, G. Miková, A.S. Luyt. Polypropylene as a potential matrix for the creation of shape stabilized phase change materials. European Polymer Journal 2007; 43:895-907. DOI:10.1016/j.europolymj.2006.12.019

6. P. Zhang, Z.W. Ma, R.Z. Wang. An overview of phase change material slurries: MPCS and CHS. Renewable and Sustainable Energy Reviews 2010; 14:598-614. DOI:10.1016/j.rser.2009.08.015
7. I. Krupa, A.S. Luyt. Thermal properties of polypropylene/wax blends. Thermochimica Acta 2001; 372:137-141. DOI:10.1016/S0040-6031(01)00450-6
8. T.N. Mtshali, I. Krupa, A.S. Luyt. The effect of cross-linking on the thermal properties of LDPE/wax blends. Thermochimica Acta 2001; 380:47-54. DOI:10.1016/S0040-6031(01)00636-0
9. H.S. Mpanza, A.S. Luyt. Comparison of different waxes as processing agents for low-density polyethylene. Polymer Testing 2006; 25:436-442. DOI:10.1016/j.polymertesting.2006.01.008
10. S.P. Hlangothi, I. Krupa, V. Djoković, A.S. Luyt. Thermal and mechanical properties of cross-linked and uncross-linked linear low-density polyethylene-wax blends. Polymer Degradation and Stability 2003; 79:53-59. DOI:10.1016/S0141-3910(02)00238-0
11. Y. Hong, G. Xin-shi. Preparation of polyethylene-paraffin compound as a form-stable solid-liquid phase change material. Solar Energy Materials and Solar Cells 2000; 64:37-44. DOI:10.1016/S0927-0248(00)00041-6
12. C. Alkan, A. Sari. Fatty acid/poly(methyl methacrylate) (PMMA) blends as form-stable phase change materials for latent heat thermal energy storage. Solar Energy 2008; 82:118-124. DOI:10.1016/j.solener.2007.07.001
13. Y. Cai, Y. Hu, L. Song, Y. Tong, R. Yang, Y. Zhang, Z. Chen, W. Fang. Flammability and thermal properties of high density polyethylene as a form-stable phase change material. Journal of Applied Polymer Science 2006; 99:1320-1327. DOI:10.1002/app.22065
14. M.J Hato, A.S. Luyt. Thermal fractionation and properties of different polyethylene/wax blends. Journal of Applied Polymer Science 2007; 104:2225-2236. DOI:10.1002/app.25494
15. Y.F. Fan, X.X. Zhang, X.C. Wang, J. Li, Q.B. Zhu. Super-cooling prevention of microencapsulated phase change material. Thermochimica Acta 2004; 413:1-6. DOI:10.1016/j.tca.2003.11.006

16. P. Zhang, Y. Hu, L. Song, J. Ni, W. Xing, J. Wang. Effect of expanded graphite on properties of high-density polyethylene/paraffin composite with intumescent flame retardant as a shape-stabilized phase change material. Solar Energy Materials and Solar Cells 2010; 94:360-365.
DOI:10.1016/j.solmat.2009.10.014
17. L. Sánchez-Silva, J.F. Rodríguez, A. Romero, A.M. Borreguero, M. Carmona, P. Sánchez. Microencapsulation of PCMs with styrene-methyl methacrylate copolymer shell by suspension-like polymerisation. Chemical Engineering Journal 2010; 157:216-222.
DOI:10.1016/j.cej.2009.12.013
18. R. Yang, Y. Zhang, X. Wang, Y. Zhang, Q. Zhang. Preparation of n-tetradecane-containing microcapsules with different shell materials by phase separation method. Solar Energy Materials and Solar Cells 2009; 93:1817-1822.
DOI:10.1016/j.solmat.2009.06.019
19. Y. Fang, S. Kuang, X. Gao, Z. Zhang. Preparation and characterization of novel nanoencapsulated phase change materials. Energy Conversion and Management 2008; 49:3704-3707.
DOI:10.1016/j.enconman.2008.06.027
20. C. Liang, X. Lingling, S. Hongbo, Z. Zhibin. Microencapsulation of butyl stearate as a phase change material by interfacial polycondensation in a polyurea system. Energy Conversion and Management 2009; 50:723-729.
DOI:10.1016/j.enconman.2008.09.044
21. G. Fang, H.Liu, F. Yang, X. Liu, S. Wu. Preparation and characterization of nano-encapsulated n-tetradecane as phase change material for thermal energy storage. Chemical Engineering Journal 2009; 153:217-221.
DOI:10.1016/j.cej.2009.06.019
22. V.V. Tyagi, S.C. Kaushik, S.K. Tyagi, T. Akiyama. Development of phase change materials based microencapsulated technology for buildings: A review. Renewable and Sustainable Energy Reviews 2011; 15:1373-1391.
DOI:10.1016/j.rser.2010.10.006
23. L. Wei, Z. Xing-Xiang, W. Xue-Chen, N. Jiang-Jin. Preparation and characterization of microencapsulated phase change material with low remnant formaldehyde content. Materials Chemistry and Physics 2007; 106:437-442.
DOI:10.1016/j.matchemphys.2007.06.030

24. A.M. Borreguero, J.L. Valverde, J.F. Rodríguez, A.H. Barber, J.J. Cubillo, M. Carmona. Synthesis and characterization of microcapsules containing Rubitherm ®RT27 obtained by spray drying. Chemical Engineering Journal 2011; 166:384-390. DOI:10.1016/j.cej.2010.10.055
25. Z. Jin, Y. Wang, J. Liu, Z. Yang. Synthesis and properties of paraffin capsules as phase change materials. Polymer 2008; 49:2903-2910. DOI:10.1016/j.polymer.2008.04.030
26. A.S. Luyt, I. Krupa. Phase change materials formed by UV curable epoxy matrix and Fischer-Tropsch paraffin wax. Energy Conversion and Management 2009; 50:57-61. DOI:10.1016/j.enconman.2008.08.026
27. X.L. Shan, J.P. Wang, X.X. Zhang, X.C. Wang. Formaldehyde-free and thermal resistant microcapsules containing n-octadecane. Thermochimica Acta 2009; 494:104-109. DOI:10.1016/j.tca.2009.04.026
28. M.N.A. Hawlader, M.S. Uddin, M.M. Khin. Microencapsulated PCM thermal-energy storage system. Applied Energy 2003; 74:195-202. DOI:10.1016/S0306-2619(02)00146-0
29. A. Sari, C. Alkan, A. Karaipekli, O. Uzun. Microencapsulated n-octacosane as phase change material for thermal energy storage. Solar Energy 2009; 1757-1763. DOI:10.1016/j.solener.2009.05.008
30. X.X. Zhang, Y.F. Fan, X.M. Tao, K.L. Yick. Fabrication and properties of microcapsules and nanocapsules. Materials Chemistry and Physics 2004; 88:300-307. DOI: 10.1016/j.matchemphys.2004.06.043
31. J. Zhao, Y. Guo, F. Feng, Q. Tong, W. Qv, H. Wang. Microstructure and thermal properties of a paraffin/expanded graphite phase-change composite for thermal storage. Renewable Energy 2011; 36:1339-1342. DOI:10.1016/j.renene.2010.11.028
32. W.L. Cheng, R.M. Zhang, K. Xie, N. Liu, J. Wang. Heat conduction enhanced shape-stabilized paraffin/HDPE composite PCMs by graphite addition: Preparation and thermal properties. Solar Energy Materials and Solar Cells 2010; 94:1636-1642. DOI: 10.1016/j.solmat.2010.05.020
33. S. Kim, J. Seo, L.D. Drzal. Improvement of electric conductivity of LLDPE based nanocomposite by paraffin coating on exfoliated graphite nanoplatelets. Composites Part A 2010; 41:581-587.

DOI:10.1016/j.compositesa.2009.05.002.

34. J.F. Su, L.X. Wang, L. Ren. Preparation and characterization of double-MF shell microPCMs used in building materials. Journal of Applied Polymer Science 2005; 97:1755-1762.
DOI:10.1002/app.21205

35. L. Sánchez, P. Sánchez, A. de Lucas, M. Carmona, J.F. Rodríguez. Microencapsulation of PCMs with a polystyrene shell. Colloid Polymer Science 2007; 285:1377-1385.
DOI:10.007/s00396-007-1696-7

36. G. Fang, Z. Chen, H. Li. Synthesis and properties of microencapsulated paraffin composites with SiO_2 shell as thermal energy storage materials. Chemical Engineering Journal 2010; 163:154-159.
DOI:10.1016/j.cej.2010.07.054

37. Y.F. Fan, X.X. Zhang, S.Z. Wu, X.C. Wang. Thermal stability and permeability of microencapsulated n-octadecane and cyclohexane. Thermochimica Acta 2005; 429:25-29.
DOI:10.1016/j.tca.2004.11.025

38. K. Cho, S.H. Choi. Thermal characteristics of paraffin in spherical capsule during freezing and melting processes. International Journal of Heat and Mass Transfer 2000; 3183-3196.
DOI:10.1016/S0017-9310(99)00329-4

39. X.X. Zhang, Y.F. Fan, X.M. Tao, K.L. Yick. Fabrication and properties of microcapsules and nanocapsules containing n-octadecane. Materials Chemistry and Physics 2004; 88:300-307.
DOI:10.1016/j.matchemphys.2004.06.043

40. L. Sánchez, P. Sánchez, M. Carmona. Influence of operation conditions on the microencapsulation of PCMs by means of suspension-like polymerization. Colloid and Polymer Science 2008; 286:1019-1027.
DOI:10.007/s00396-008-1864-4

41. X.X. Zhang, Y.F. Fan, X.M. Tao, K.L. Yick. Crystallization and prevention of supercooling of microencapsulated n-alkanes. Journal of Colloid and Interface Science 2005; 281:299-306.
DOI:10.1016/j.jcis.2004.08.046

42. S. Alay, C. Alkan, F. Göde. Synthesis and characterization of poly(methyl methacrylate)/n-hexadecane microcapsules using different cross-linkers and their application in some fabrics. Thermochimica Acta 2011; 518:1-8.
DOI:10.1016/j.tca.2011.01.014
43. L. Xiao-Zheng, T. Zhi-Cheng, Z. Guang-Long, S. Li-Xian, Z. Tao. Microencapsulation of n-eicosane as energy storage material. Chinese Journal of Chemistry 2004; 22:411-414.
44. H. Zhang, X. Wang. Fabrication and performances of microencapsulated phase change materials based on n-octadecane core and resorcinol-modified melamine-formaldehyde shell. Colloids and Surfaces A: Physicochemical and Engineering Aspects 2009; 332:129-138.
DOI:10.1016/j.colsurfa.2008.09.013
45. M. Xiao, B. Feng, K. Gong. Thermal performance of a high conductive shape-stabilized thermal energy storage material. Solar Energy Materials and Solar Cells 2001; 69:293-296.
DOI:10.1016/S0927-0248(01)00056-3
46. Ç. Gökhan, S. Küsefoğlu. Thermal and mechanical behavior of unsaturated polyesters filled with phase change material. Journal of Applied Polymer Science 2006; 100:832-838.
DOI:10.1002/app.23181
47. L. Xia, P. Zhang, R.Z. Wang. Preparation and thermal characterization of expanded graphite/paraffin composite phase change material. Carbon 2010; 48:2538-2548.
DOI:10.1016/j.carbon.2010.03.030
48. A. Shulkin, H.D.H. Stöver. Polymer microcapsules by interfacial polyaddition between styrene-maleic anhydride copolymers and amines. Journal of Membrane Science 2002; 209:421-432.
DOI:10.1016/S0376-7388(02)00348-4
49. N. Sarier, E. Onder. The manufacture of microencapsulated phase change materials suitable for the design of thermally enhanced fabrics. Thermochimica Acta 2007; 452:149-160.
DOI:10.1016/j.tca.2006.08.002
50. D. Juárez, S. Ferrand, O. Fenollar, V. Fombuena, R. Balart. Improvement of thermal inertia of styrene-ethylene/butylene-styrene (SEBS) polymers by addition of

microencapsulated phase change materials (PCMs). European Polymer Journal 2011; 47:153-161.
DOI:10.1016/j.eurpolymj.2010.11.004

51. Y. Jiang, D. Wang, T. Zhao. Preparation, characterization, and prominent thermal stability of phase change-change microcapsules with phenolic resin shell and n-hexadecane core. Journal of Applied Polymer Science 2007; 104:2799-2806.
DOI:10.1002/app.25962

52. J.A. Molefi, A.S. Luyt, I. Krupa. Comparison of LDPE, LLDPE and HDPE as matrices for phase change materials based on a soft Fischer-Tropsch paraffin wax. Thermochimica Acta 2010; 500:88-92.
DOI:10.1016/j.tca.2010.01.002

Chapter 3: Materials and methods

3.1 Materials

3.1.1 Polypropylene (PP)

Isotactic polypropylene was supplied in pellet by Sasol Polymers, South Africa. It has an MFI of 10 g min^{-1}, specific enthalpy of melting of 90 J g^{-1}, melting temperature of 163-165 °C, and a density of 0.901 g cm^{-3}.

3.1.2 M3 paraffin wax

Soft paraffin wax (M3 wax) was supplied in powder form by Sasol Wax. It is a paraffin wax consisting of approximately 99% of straight chain hydrocarbons and few branched chains. It has an average molar mass of 440 g mol^{-1} and a carbon distribution between C15 and C78. Its density is 0.90 g cm^{-3} and it has a melting point range around 40-60 °C.

3.1.3 Styrene monomer

Reagent grade (99%) styrene monomer was supplied in liquid form by Sigma-Aldrich, South Africa. It has a density of 0.909 g cm^{-3}.

3.1.4 Other chemicals

3.1.4.1 2,2'-Azobis (2-methylpropionitrile) (AIBN)

2,2'-Azobis (2-methylpropionitrile) (AIBN) was supplied in liquid form by Sigma-Aldrich, South Africa. It has a density of 0.858 g cm^{-3}, its chemical formula is $C_8H_{12}N_4$ and it was used as an iniator.

3.1.4.2 n-Dodecyl mercaptan (DDM)

n-Dodecyl mercaptan was supplied in liquid form by Sigma Aldrich, South Africa. It was used as a chain transfer agent and it has a density of 0.845 g cm^{-3}.

3.1.4.3 Sodium lauryl sulphate (SLS)

Sodium lauryl sulphate (90% assay) was supplied in powder form by Merck chemicals, South Africa. It was used as an emulsifier and its chemical formula is $CH_3(CH_2)_{11}OSO_3Na$.

3.1.4.4 Polystyrene-block-poly(ethylene-ran-butylene)-block-polystyrene (SEBS)

Polystyrene–block–poly(ethylene-ran-butylene)-block-polystyrene was supplied in powder form by Sigma-Aldrich, South Africa. It was used as a compatibilizer, has a density of 0.91 g cm^{-3} and a molecular weight of 118000 g mol^{-1}.

3.1.4.5 Sodium hydroxide (NaOH)

Sodium hydroxide was supplied in pellet form by Sigma-Aldrich, South Africa. It was a chemically pure (CP) grade with an assay of 99%, and a density of 2.13 g cm^{-3}. It was used to wash the styrene monomer before it was used.

3.1.4.6 Methanol (CH_3OH)

Methanol was supplied in liquid form by Associated Chemical Enterprises (ACE), South Africa. The methanol with a density of 0.79 g cm^{-3} was used to wash polystyrene microcapsules after polymerization.

3.2 Treatment of styrene monomer

Styrene monomer was washed three times with an aqueous solution of 10 wt% sodium hydroxide and then with deionized water in order to remove the inhibitor. The styrene solution was poured into the calcium chloride powder used as a desiccant (state of extreme dryness).

3.3 Preparation of PCM microcapsules

The suspension polymerization reactions were performed in a 1000 mL three neck-flask, equipped with digital control of stirring rate and temperature, a reflux condenser and a nitrogen gas inlet tube. The synthesis process involved two phases (Table 3.1): (i) continuous phase containing water and sodium lauryl sulphate, and (ii) discontinuous phase containing M3 paraffin wax, styrene, 2,2-azobis(2-methylpropionitrile), and n-dodecyl mercaptan. The continuous phase was transferred to the flask with mild agitation (150 rpm). According to the continuous phase, emulsions are distinguished between oil-in-water (o/w) and water-in-oil (w/o) systems. The paraffin/water emulsion is an o/w emulsion where fine paraffin droplets are dispersed in water and the surfactant molecules are adsorbed at the interface between the paraffin and water as shown in Figure 3.1.

Table 3.1 Recipe for the obtaining of microcapsules containing M3 paraffin wax and experimental conditions used

	Ingredients	**Measure**
Continuous phase / g	Water	377
	Sodium lauryl sulphate	3.77
Discontinuous phase / g	M3 paraffin wax	25
	2.2-Azobis(2-methylpropionitrile)(AIBN)	0.1
	n-Dodecyl mercaptan (DDM)	0.08
	Styrene	75
Reaction temperature / °C		90
Stirring rate / rpm		900
Reaction time / h		5

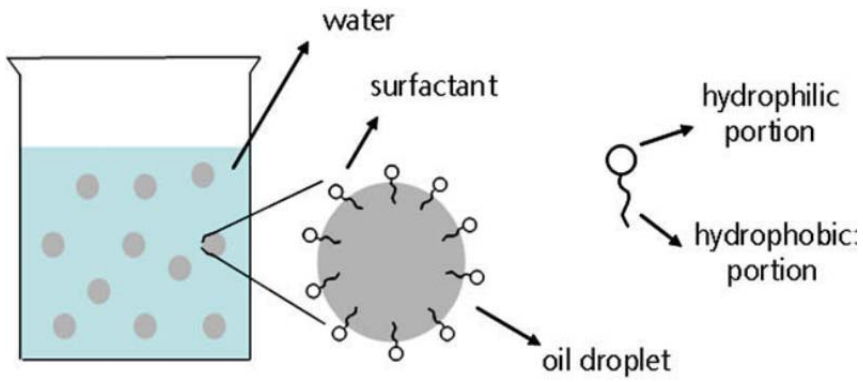

Figure 3.1 Illustration of an o/w emulsion [1]

The discontinuous phase was then added to the continuous phase with vigorous stirring (900 rpm) at a constant temperature of 75 °C. The polymerization process was continued for 3-5 hours under nitrogen atmosphere. After formation, the microcapsules were washed five times with methanol and filtered under vacuum to remove impurities. The purified microcapsules were dried at 35 °C for 24 hours. The process was repeated several times to obtain sufficient PCM polystyrene microcapsules to be mixed into the polypropylene matrix in a Brabender 55 mL mixer.

3.4 Blends preparation

The sample ratios are shown in Table 3.2. All the samples were prepared by melt-mixing using a Brabender Plastograph 55 mL internal mixer. Prior to processing, all the materials were dried for 12 h under vacuum at 80 °C. Two different mixing procedures were applied: firstly, PP/SEBS were prepared for 5 min at 170 °C and a rotor speed of 45 rpm to make sure that SEBS is uniformly distributed in the PP before mixing with PS. PS was then blended with PP/SEBS for 10 min under the same processing conditions. The same procedure was followed where PS:wax microcapsules instead of pure PS was used. This two-step mixing procedure had been widely used by other researchers and proved to be necessary for SEBS to migrate to and distribute between the phase boundaries and effectively compatibilize the blends. The samples were then melt-pressed at 170 °C for 10 min under 50 kPa pressure using a hydraulic melt-press to form 15 x 15 cm^2 square sheets. Test samples were then cut from the sheets for the various analyses.

Table 3.2 Sample ratios used for the preparation of the different blends

PP (w/w)	PP/PS (w/w)	PP/PS/SEBS (w/w/w)
100	90/10	82.5/10/7.5
-	80/20	72.5/20/7.5
-	70/30	62.5/30/7.5
-	60/40	52.5/40/7.5
PP (w/w)	**PP/PS:M3 wax (w/w)**	**PP/PS:M3 wax/SEBS**
100	90/10	82.5/10/7.5
-	80/20	72.5/20/7.5
-	70/30	62.5/30/7.5
-	60/40	52.5/40/7.5

3.5 Sample analysis

3.5.1 Dynamic mechanical analysis (DMA)

DMA can simply be defined as applying an oscillating force to a sample and analyzing the material's response to that force. DMA supplies an oscillatory force, causing a sinusoidal stress to be applied to the sample, which generates a sinusoidal strain. By measuring both the amplitude of the deformation at the peak of the sine wave and the lag between the stress and the strain sine waves, quantities like the modulus, the viscosity, and the damping can be calculated [2-5].

The dynamic mechanical properties of the blends were investigated using a Perkin Elmer Diamond DMA. The settings for the analyses were as follows:

Frequency	1 Hz
Amplitude	20 μm
Temperature range	-110 to 140 °C
Temperature program mode	Ramp
Measurement mode	Bending (dual cantilever)

Heating rate	5 °C min^{-1}
Preloading force	0.02 N
Sample length	20 mm
Sample width	12.0 – 12.5 mm
Sample thickness	1.0 – 1.3 mm

3.5.2 Differential scanning calorimetry (DSC)

DSC is a technique in which the change of the difference in the heat flow rate to the sample and to a reference sample is analyzed while they are subjected to a temperature programme. There are two basic types of DSC. These are (i) power-compensated DSC, where the sample and reference are heated by separate individual heaters, and the temperature difference is kept close to zero; and (ii) heat flux DSC, where the sample and the reference are heated from the same source and the temperature difference is measured. This signal is converted to a power difference using the calorimetric sensitivity. Physical changes in the sample that may be measured by DSC include melting temperature (T_m), crystallization temperature (T_c), glass transition temperature (T_g), and degradation or decomposition temperature (T_d) [6-8].

DSC analyses were done in a Perkin Elmer Pyris-1 differential scanning calorimeter under flowing nitrogen (flow rate 20 mL min^{-1}). The instrument was computer controlled and the peak analyses were done using Pyris software. The instrument was calibrated using the onset temperatures of melting of indium and zinc standards, as well as the melting enthalpy of indium. Samples of mass 5-10 mg were sealed in aluminium pans and heated from -30 to 190 °C at a heating rate of 10 °C min^{-1}, and cooled under the same conditions. The peak temperatures of melting and crystallization, as well as the melting and crystallization enthalpies, were determined from the second heating scan. All the DSC measurements were repeated three times for each sample. The temperatures and enthalpies are reported as average values with standard deviations.

3.5.3 Thermogravimetric analysis (TGA)

Thermogravimetric analysis is a technique in which the change in the sample mass is analysed while the sample is subjected to a temperature programme. TGA is mainly used to

characterize the decomposition and thermal stability of materials under different conditions, and to examine the kinetics of physico-chemical processes occurring in the sample [8].

The TGA analyses in this study were carried out in a Perkin Elmer TGA7 thermogravimetric analyzer. Samples ranging between 5 and 10 mg were heated from 30 to 600 °C at a heating rate of 10 °C min^{-1} under nitrogen (flow rate 20 mL min^{-1}).

3.5.4 Scanning electron microscopy (SEM)

In SEM a fine probe of electrons with energies typically up to 40 keV is focused on a specimen, and scanned along a pattern of parallel lines. Various signals are generated as a result of the impact of the incident electrons, which are collected to form an image or to analyse the sample surface. These are mainly secondary electrons, with energies of a few tens of eV, high-energy electrons backscattered from the primary beam and characteristic X- rays [9]. In SEM the nature of the sample determines the preparation of the sample, since appropriate samples may be examined directly with little or no prior preparation. Unfortunately, most polymers present specific problems making them inappropriate. Therefore proper sample preparation is necessary prior to characterization, and these include (i) plasma etching, (ii) conductive coatings through evaporation or sputtering; and (iii) chemical etching methods [4].

To determine the morphology of the fractured surfaces in this study, a Shimadzu ZU SSX-550 Superscan scanning electron microscopy was used and the analysis was done at room temperature. The samples were fractured by freezing them in liquid nitrogen, and simply breaking the specimen into appropriate size to fit the specimen chamber. The fractured samples were gold coated by sputtering to produce conductive coatings onto the samples. The fracturing of samples by liquid nitrogen was done only for the blends (PP/PS: M3 wax), but since PS:wax was in powder form there was no need for fracturing, but the samples were gold coated by sputtering before recording the SEM micrographs.

3.5.5 Tensile testing

When considering the mechanical properties of polymeric materials, and in particular when designing a tensile testing method, the parameters most generally considered are stress, strain

and Young's modulus. Stress is defined as the force applied per unit cross sectional area and has the basic dimensions of N m^{-2} in SI units. Strain is the increase in length of the specimen per original length and it is dimensionless. The ratio of stress to strain is known as the Young's modulus and this parameter has the dimensions of force per unit area [10].

A Hounsfield H5KS universal testing machine was used for the tensile analysis of the samples. The dumbbell shaped samples (Figure 3.2) with a Gauge length of 24 mm, a thickness of 2 mm and width between 4.7 and 5.0 mm were tested at a speed of 20 mm min^{-1}. About five test specimens for each sample were analysed, and the averages and standard deviations of the different tensile properties are reported.

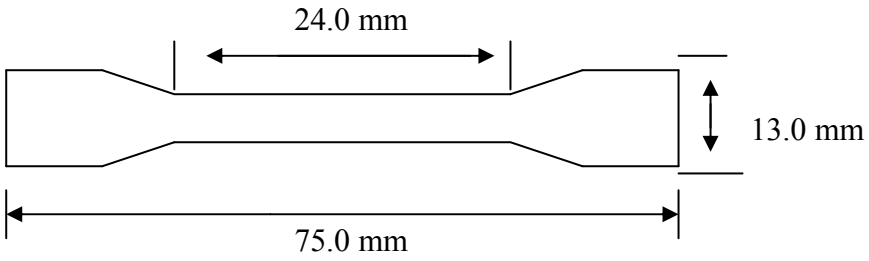

Figure 3.2 Dumbbell shaped tensile testing sample

3.5.6 Thermal conductivity

The method used for measuring thermal conductivity and diffusivity of materials is the transient plane source (TPS) technique, which is also called the hot disk (HD) technique. The method is based on the use of a transiently heated plane sensor, and is in its most common adaptation referred to as the Hot Disk Thermal Constants Analyzer. The hot disk sensor consists of an electrically conducting pattern in the shape of a double spiral, which has been etched out of thin metal (nickel) foil. The main advantages of the hot disk are accuracy, wide range of conductivity measurement, the production of results in a relatively short time (10 s to 10 min), and the use of different sensor sizes to accommodate different sample types. The important requirement on the geometry of the sample is that the surface facing the sensor should be fairly plane [11].

The thermal conductivity in this study was carried out on a Hot Disk TPS 500. It is easier to make measurements on larger than on smaller samples. In order to determine both the thermal conductivity and thermal diffusivity with good accuracy, the thickness of a sample should preferably not be less than the radius of the hot disk sensor. In this study the hot disk sensor had a diameter of about 6-7 mm and samples with thickness of 10 mm and diameter of 70 mm were used for the analysis. The hot disk sensor was placed between the plane surfaces of two sample pieces (the samples are of the same composition) of the material under investigation. The basic assumption of the theory for this experimental technique is that the sensor is located in an infinite material. The conductivity measurements were carried out in a relatively short time and before measurements were taken the samples were kept at the same ambient temperature long enough (15 minutes) to avoid any temperature drift before and during the experiment. All measurements were repeated three times for each sample.

3.3.7 Fourier-transform infrared (FTIR) spectroscopy

Fourier-transform infrared spectroscopy is a technique for identifying types of chemical bonds in a molecule by producing an infrared absorption spectrum that is like a molecular "fingerprint". The chemical bonds can be either organic or inorganic, and it can give important information about the structure of organic molecules. It can be utilized to identify compounds and investigate sample composition, as well as interactions/reactions between functional groups on the different components in polymer blends and composites [12].

FTIR spectroscopy was performed using a Perkin Elmer Spectrum 100 infrared spectrometer. PS:wax microcapsules were analysed in an attenuated total reflectance (ATR) detector over a 400-4000 cm^{-1} wavenumber range at a resolution of 4 cm^{-1}.

3.8 References

1. L. Huang, M. Petermann, C. Doetsch. Evaluation of paraffin/water emulsion as a phase change slurry for cooling applications. Energy 2009; 34:1145-1155. DOI:10.1016/j.energy.2009.03.016
2. K.P. Menard. Dynamic Mechanical Analysis: A Practical Introduction. CRC Press LLC, New York (1999) p.13-20.

3. H. Lu, Y. Obeng, K.A. Richardson. Applicability of dynamic mechanical analysis for CMP polyurethane pad studies. Materials Characterization 2003; 49:177-186. DOI:10.1016/S1044-5803(03)00004-4
4. F. Oulevey, N.A. Burnham, G. Gremand, A.J. Kulik, H.M. Pollock, A. Hammiche, M. Reading, M. Song, D.J. Hourston. Dynamic mechanical analysis at the submicron scale. Polymer 2000; 41:3087-3092. DOI:10.1016/S0032-3861(99)00601-1
5. P.S. Thomas, S. Thomas, S. Bandyopadhyay, A. Wurm, C. Schick. Polystyrene/calcium phosphate nanocomposites: Dynamic mechanical and differential scanning calorimetric studies. Composites Science and Technology 2008; 68:3220-3229. DOI:10.1016/j.compscitech.2008.08.008
6. W. Hemminger, S.M. Sarge. Definitions, nomenclature, terms and literature. In: M.E. Brown (Editor). Handbook of Thermal Analysis and Calorimetry, Volume 1. Principles and Practice, Elsevier Science, Amsterdam (1998) p.8-16.
7. G.B. McKenna, S.L. Simon. The glass transition: Its measurement and underlying physics. In: S.Z.D. Cheng (Editor). Handbook of Thermal Analysis and Calorimetry, Volume 3. Applications to Polymers and Plastics, Elsevier Science, Amsterdam (2002) p.85-92.
8. B. Wunderlich. Thermal Analysis of Polymeric Materials. Springer-Verlag, Berlin (2005) p.279-438.
9. A. Bogner, P.H. Jouneau, G. Thollet, D. Basset, C. Gauthier. A history of scanning electron microscopy developments: Towards "Wet-STEM" imaging. Micron 2007; 38:309-401. DOI:10.1016/j.micron.2006.06.008
10. J.W. Nicholson. The Chemistry of Polymers, 3rd Edition. The Royal Society of Chemistry, Cambridge (2006) p.95.
11. Preparation and thermal characterization of expanded graphite/paraffin composite phase change material. Carbon 2010; 48:2538-2548. DOI:10.1016/j.carbon.2010.03.030
12. B. Stuart. Infrared Spectroscopy: Fundamentals and Applications. John Wiley and Sons, Chichester (2004) p.23.

Chapter 4: Results and discussion

4.1 Scanning electron microscopy (SEM)

The SEM images of the microencapsulated PCM are shown in Figure 4.1. The particles have irregular spherical shapes and their sizes are in the range 16-24 μm. In other SEM images of microcapsules, prepared by using different core and shell materials [1-4], the appearance of the microcapsules was similar.

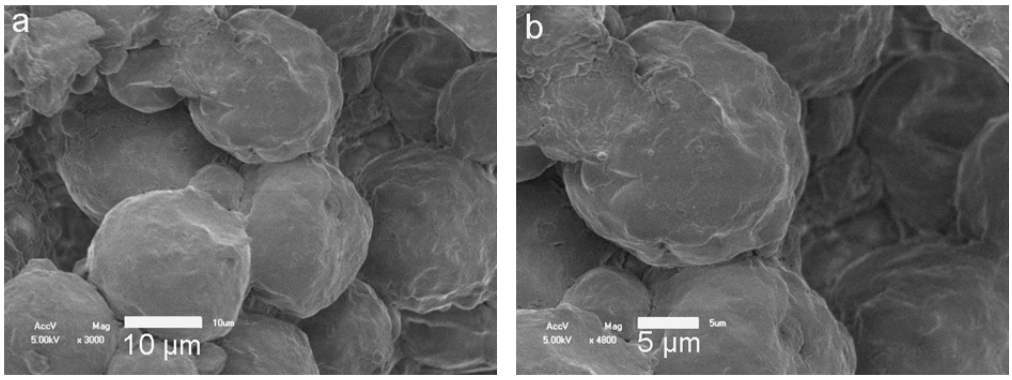

Figure 4.1 SEM micrographs of PS:wax capsules ((a) 3000x magnification & (b) 4800x magnification)

Figure 4.2 shows the SEM images of the PP/(PS:wax) blends at different compositions. The PS:wax microcapsules are fairly well dispersed in the PP matrix, and they are mostly intact. Only one of the photos (Figure 4.2a) shows a microcapsule with a ruptured PS skin (arrow A). The presence of a core and a thin shell is clear from this image, indicating the successful encapsulation of the wax. Li *et al*. [5], who studied micro-encapsulated paraffin/HDPE/wood flour composites as form stable PCMs for thermal energy storage, also observed that most of the microencapsulated particles in the form-stable PCM were still intact, though some of them were ruptured.

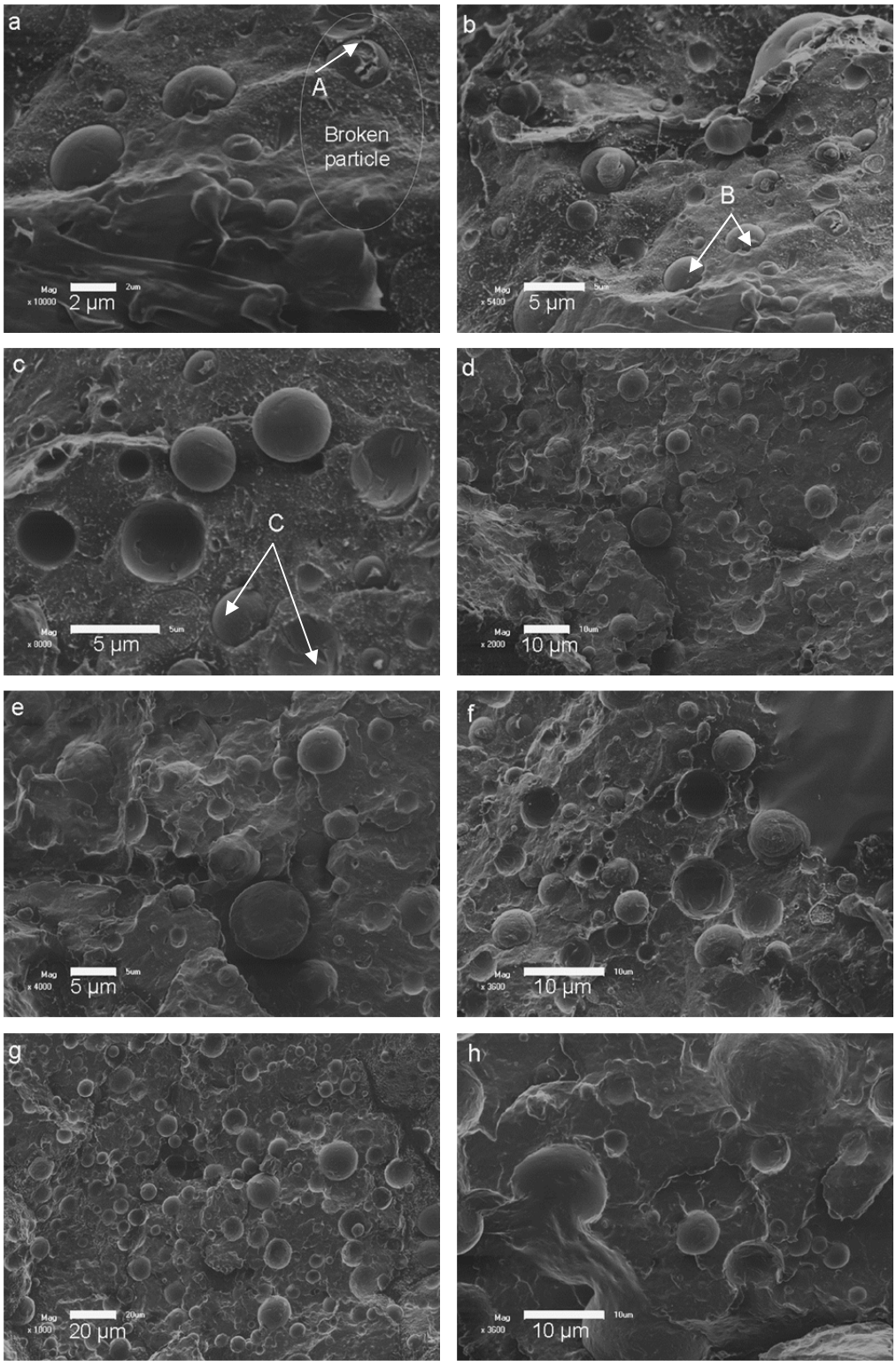

Figure 4.2 SEM micrographs of 90/10 w/w PP/(PS:wax) ((a) 10000x magnification & (b) 5400x magnification), 80/20 w/w PP/(PS:wax) ((c) 8000x magnification & (d) 2000x magnification), 70/30 w/w PP/(PS:wax) ((e) 4000x magnification & (f) 3600x magnification), and 60/40 w/w PP/(PS:wax) ((g) 1000x magnification & (h) 3600x magnification)

The SEM images of the unmodified PP/(PS:wax) blends generally show PCM microcapsules embedded in the PP matrix (Figure 4.2b, arrow B and Figure 4.2c, arrow C). However, in Figure 2c we observe that there are microcapsules that are clearly not embedded in the matrix, but they are still attached to the matrix even after liquid nitrogen fracturing. This can be attributed to fairly good interaction between the microcapsules and the matrix, even in the absence of SEBS modification. Moreover, the microcapsules in these images are obviously smaller (1-8 μm), smoother and more spherical than the particles shown in Figure 4.1. This indicates that the PS:wax microparticles were agglomerated before mixing them with the polymer. The breaking up of the agglomerates into individual microcapsules and fairly well dispersion of the microcapsules in the PP matrix during melt mixing, is further evidence of the fairly good interaction between the microcapsules and the matrix.

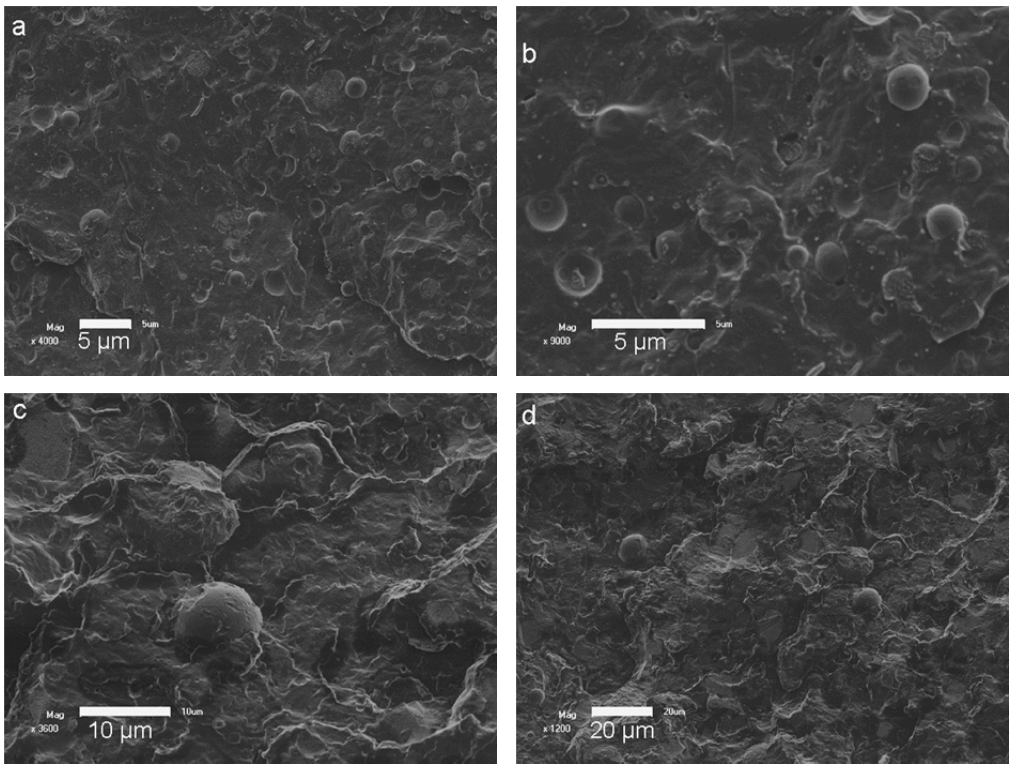

Figure 4.3 SEM micrographs of 62.5/30/7.5 w/w PP/(PS:wax)/SEBS ((a) 4000x magnification & (b) 5000x magnification), and 52.5/40/10 w/w PP/(PS:wax)/SEBS ((c) 3600x magnification & (d) 1200x magnification)

Figure 4.3 shows the SEM images of PP/(PS:wax) modified with 7.5% of styrene-ethylene/butylene-styrene (SEBS). The presence of SEBS obviously increased the adhesion between the PS:wax microcapsules and the PP matrix. This is observable from the clear coverage of the embedded PS:wax microparticles by the PP matrix. This improvement in

interfacial adhesion is attributed to the nature of the compatibilizer. The PS and EB blocks of the SEBS are respectively miscible with PS and PP. Similar results were obtained by Ismail *et al.* [6], who studied the morphology of an uncompatibilized and a compatibilized polystyrene/polypropylene blend using various compatibilizers such as ethylene vinyl acetate, SEBS, Surlyn and sodium salt hydrate of 4-styrene sulfonic acid at concentrations of 7.5%. The incorporation of SEBS into the PP/PS blends resulted in a finer degree of dispersion of the particles and morphological evidence of interfacial adhesion.

4.2 Fourier transform-infrared spectroscopy (FT-IR)

The FT-IR spectra of wax, polystyrene and microencapsulated PCM are shown in Figure 4.4. For wax the absorption peaks at 2916-2848 cm^{-1} are characteristic of the aliphatic C-H stretching vibration, the peak at 1462 cm^{-1} is with the C-H bending vibration and the peak at 718 cm^{-1} with the in-plane rocking vibration of the CH_2 group. For polystyrene the absorption peaks at 3000-3030 cm^{-1} are associated with the aromatic C-H stretching vibration, the absorption peak at 2930 cm^{-1} with the aliphatic C-H stretching vibration, the peaks at 1600 and 1495 cm^{-1} with the benzene ring C=C stretching vibration, and the peaks at 750-700 cm^{-1} with the benzene ring deformation vibration. The FT-IR spectrum of the microcapsules is almost exactly the same as that of the polystyrene, which indicates that the microcapsules are mostly intact and that the FTIR only detected the polystyrene shell.

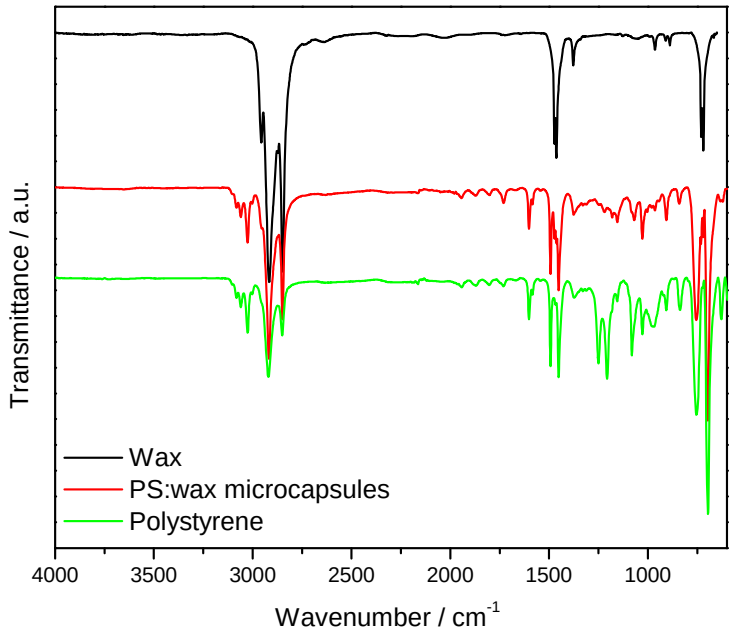

Figure 4.4 FTIR spectra of wax, PS and microencapsulated PCM

4.3 Thermogravimetric analysis (TGA)

The TGA curves of all the samples are shown in Figures 4.5 to 4.8. The thermal stabilities of the samples were characterized in terms of the temperatures at 20 and 60% mass loss. A summary of the TGA results is presented in Table 4.1.

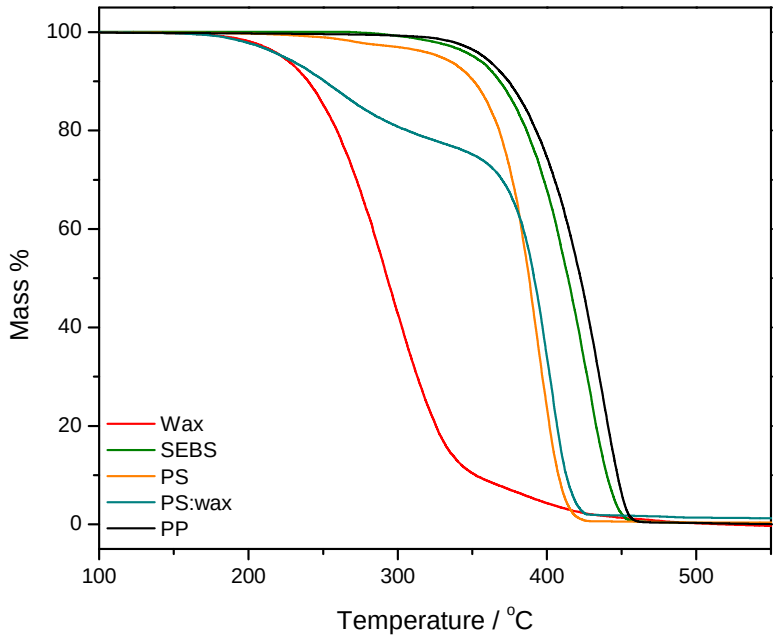

Figure 4.5 TGA curves of PP, SEBS, PS, PS:wax and wax

The TGA curves of the neat materials (PP, wax, SEBS, PS and the PS:wax microcapsules) are shown in Figure 4.5. The PP, wax, SEBS and PS decompose completely in a single step, whereas the PS:wax microcapsules exhibits a two-step degradation. The PP has the highest thermal stability, followed by the SEBS, the PS, the PS:wax microcapsules and then the wax. In the TGA curve of the PS:wax microcapsules the first weight loss (20 wt%) at temperatures around 230 °C is attributed to the evaporation of the paraffin wax. At temperatures higher than 300 °C there is a second weight loss step of 80 wt%; this is related to the decomposition of polystyrene. The results show that only 20% of the microcapsules consisted of wax, while the remaining 80% consisted of the polystyrene shell. This will be a drawback if the system is to be used as a phase-change material, where a high wax concentration is needed. Sánchez *et al.* [7] reported microencapsulation of PCMs with a polystyrene shell and observed three degradation steps from the TGA plot. The first weight loss below 100 °C was because of the elimination of methanol and water (drying of surface wetting agents), the one between 120

and 250 °C was attributed to the paraffin wax. At temperatures higher than 300 °C the weight loss was due to polystyrene.

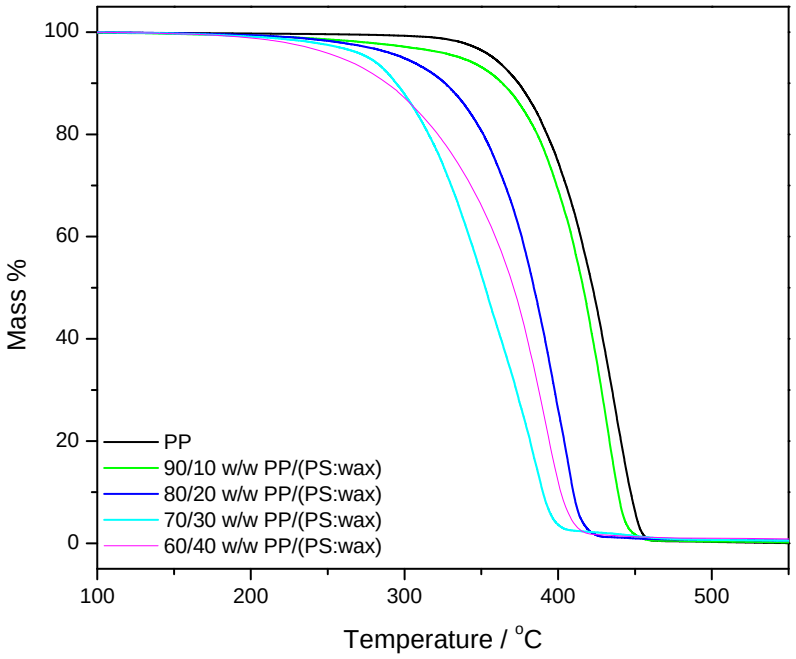

Figure 4.6 TGA curves of wax, PP and PP/(PS:wax) blends

The TGA curves for PP and the PP/(PS:wax) blends are shown in Fig. 4.6. The results show that the thermal stability of the blends decreases with an increase in PS:wax microcapsules contents as a consequence of lower thermal stability of both the wax and PS. Since the wax does not decompose but only evaporates, the degradation of PS probably provides free radicals that initiate the decomposition of the PP chains. It is interesting that the blends decompose in only one distinguishable step, whereas the TGA curve for the PS:wax clearly shows two mass loss steps. This is probably due to (i) both PP and PS acting as heat isolators so that it takes longer for heat to reach the wax chains, and (ii) the time it takes for the wax volatiles to diffuse to the surface of the molten blend.

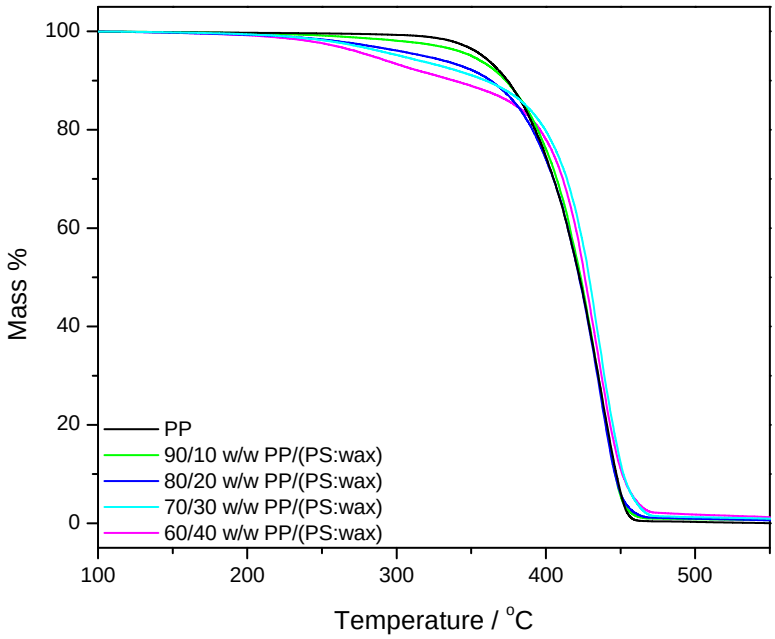

Figure 4.7 TGA curves of PP, wax and PP/(PS:wax)/SEBS blends

Figure 4.7 depicts the TGA curves of the PP/(PS:wax)/SEBS blends. It is clear from the curves and Table 4.1 that all the blends compatibilized with SEBS are thermally more stable than the unmodified blends at the same (PS:wax) contents. The more thermally stable SEBS seems to act as a heat barrier so that it takes longer for heat to reach the (PS:wax) microcapsules, and the interaction between SEBS seems to retard the degradation of PS. The development of a separate mass loss step on the lower temperature side of the main mass loss step is probably the result of wax evaporation that starts before PS degradation. For example, for the 52.5/40/7.5 w/w PP/(PS:wax)/SEBS sample the mass loss associated with the first step is about 8%. The results in Figure 4.5 show that the wax forms about 20 wt% of the microcapsules, and if the microcapsules content is 40 wt% of the blend, then the wax forms about 8 wt% of the blend.

The blends of PP/PS and PP/PS/SEBS were also investigated (Figure 4.8). The results show that the effectiveness of SEBS in enhancing the compatibility of the blends depends on the blend composition. A significant improvement in thermal stability is observed on addition of 7.5% SEBS into 90/10 PP/PS blend. However, not much improvement in thermal stability is observed upon addition of 7.5% to the 70/30 PP/PS blend. This confirms that the interaction

between SEBS and PS retards the degradation of PS, because for the 62.5/30/7.5 w/w PP/PS/SEBS sample there is not enough SEBS to associate with all the PS in the blend.

Table 4.1 TGA results for PP, wax, PS, PS:wax, and the different investigated blends

Sample	$T_{20\%}$ / °C	$T_{60\%}$ / °C
PP	392.2	429.2
Wax	258.7	300.6
SEBS	384.1	422.8
PS	366.4	390.6
PS:wax	292.4	398.7
PP/(PS:wax) (w/w)		
90/10	388.2	422.3
80/20	350.8	388.2
70/30	315.1	363.8
60/40	321.6	380.1
PP/PS:wax/SEBS (w/w)		
82.5/10/7.5	393.1	427.2
72.5/20/7.5	385.7	426.1
62.5/30/7.5	398.3	438.7
52.5/40/7.5	393.3	431.1

$T_{20\%}$ and $T_{60\%}$ are the degradation temperatures at 20 and 60% mass loss respectively

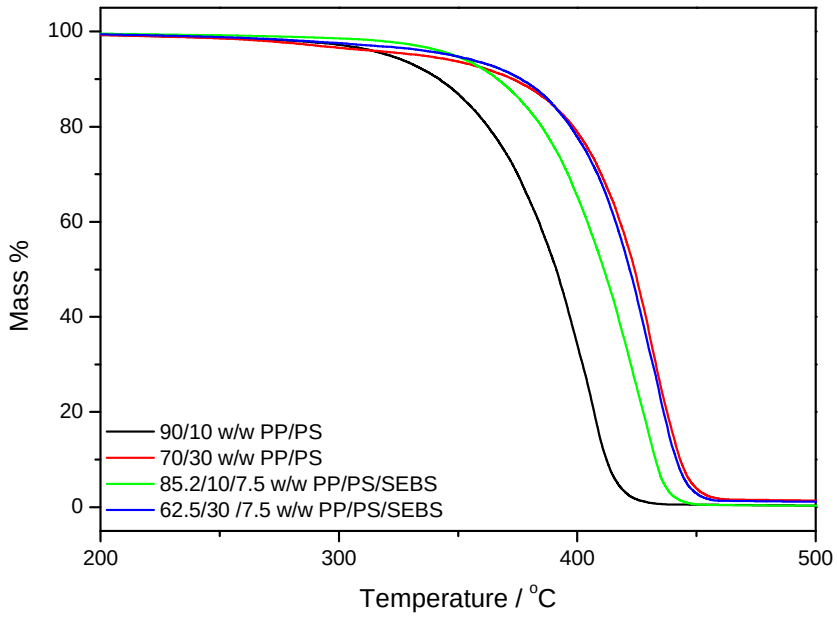

Figure 4.8 TGA curves of PP, PP/PS and PP/PS/SEBS blends

4.4 Differential scanning calorimetry (DSC)

The DSC results for the PS:wax microcapsules, PP/(PS:wax) and the PP/(PS:wax)/SEBS blends are summarized in Figures 4.9 to 4.15. The peak temperatures of melting, melting enthalpies and the calculated melting enthalpies are summarized in Table 4.2 for the PS:wax microcapsules containing systems. All the reported DSC heating and cooling results were obtained from the second scan to eliminate the effect of thermal history. The calculated melting enthalpy values of PP were determined from Equation 4.1.

$$\Delta H^{calc} = \Delta H_{m,PP} \times w_{pp} \qquad (4.1)$$

where ΔH_m^{calc} is the calculated melting enthalpy of PP in the blend, and $\Delta H_{m,PP}$ is melting enthalpy of neat PP, and w_{pp} is the weight fraction of PP in the blend. In this calculation it is assumed that the PS or PS:wax microcapsules do not have any influence on the crystallization behaviour of PP.

The DSC curves of the microcapsules and pure wax are shown in Figure 4.9. The wax shows a melting peak at 59 °C, with a peak shoulder at 33 °C and a phase change enthalpy of 149 J g^{-1}. The peak shoulder relates to a solid-solid transition, and the main peak is associated with the melting of the crystallites [15-16]. The DSC curve of the microcapsules shows a peak in the same temperature range as that of the pure wax. It also shows a small peak between 80 and 90 °C which is probably due to the glass transition of PS. The transition enthalpy of the microcapsules is 40 J g^{-1}, which means that the microcapsules contained only 28% wax. Similar results were obtained by Alkan *et* a.l [17] who studied the preparation, characterization, and determination of the thermal properties of PMMA microencapsulated docosane as PCM for thermal energy storage. They observed that the PMMA/docosane microcapsules consisted of an average of 28 wt% docosane. This value is slightly higher than the 20% calculated from the TGA results (section 4.3). The results show that the PCM storage capacity is severely reduced by encapsulation in PS.

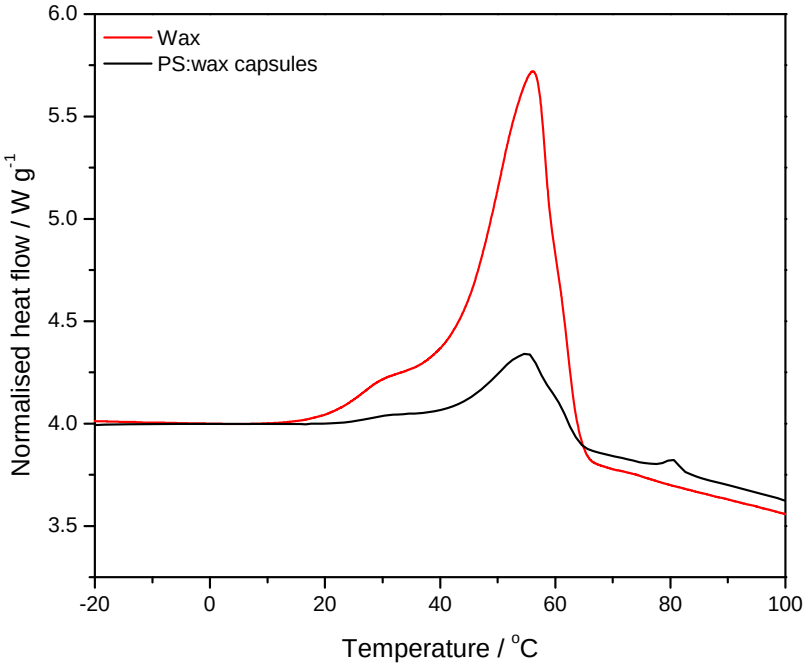

Figure 4.9 DSC heating curves of PS:wax microcapsules and wax

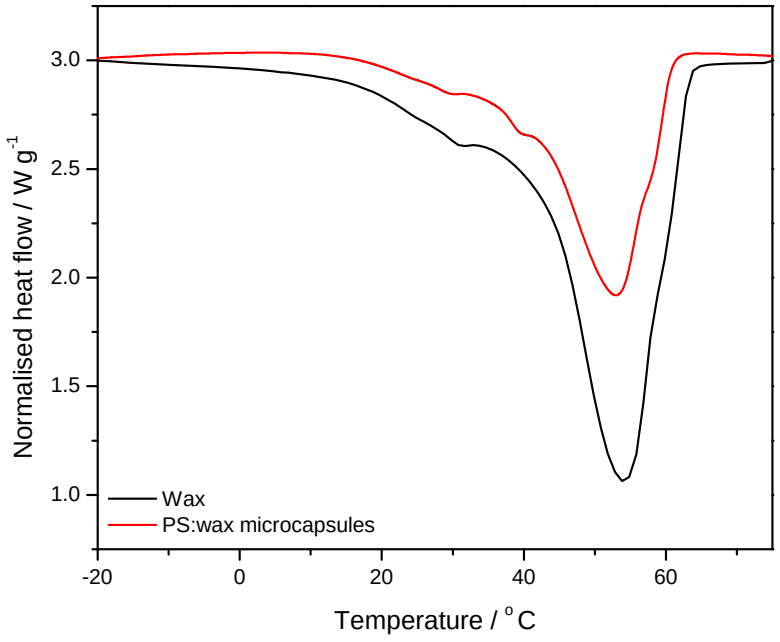

Figure 4.10 DSC cooling curves of PS:wax microcapsules and wax

Table 4.2 Summary of the DSC heating results for all the investigated samples

Sample	$T_{p,m}$(PP) / °C	ΔH_m^{obs}(PP) / J g^{-1}	ΔH_m^{calc}(PP) / J g^{-1}	$T_{p,m}$(wax) / °C	ΔH_m^{obs}(wax) / J g^{-1}
PP	169.9 ± 0.9	83.3 ± 0.3			
PS:wax				53.3 ± 1.5	40.3 ± 5.2
Wax				58.8 ± 1.0	148.5 ± 0.3
PP/(PS:wax)					
90/10	164.2 ± 0.7	64.3 ± 4.3	75.0		
80/20	162.2 ± 0.6	62.6 ± 1.5	66.6	55.5 ± 2.0	6.1 ± 0.3
70/30	160.1 ± 0.6	57.2 ± 1.3	58.3	56.9 ± 2.1	13.6 ± 2.1
60/40	158.2 ± 1.2	44.5 ± 1.1	50.0	56.3 ± 1.8	16.1 ± 2.0
PP/(PS:wax)/SEBS					
82.5/10/7.5	164.1 ± 0.3	62.6 ± 1.9	68.7		
72.5/20/7.5	159.1 ± 2.3	54.5 ± 0.7	60.4	53.2 ± 2.1	5.1 ± 0.1
62.5/30/7.5	158.3 ± 2.2	40.5 ± 0.4	52.1	50.9 ± 0.3	11.9 ± 0.5
52.5/40/7.5	157.6 ± 0.4	39.9 ± 0.5	43.7	54.8 ± 0.5	14.9 ± 0.2

$T_{p,m}$, ΔH_m^{obs}, and ΔH_m^{add} are respectively the peak temperature of melting, observed melting enthalpy, and calculated melting enthalpy.

The DSC cooling curves of neat wax and the PS:wax microcapsules are presented in Figure 4.10. The pure wax shows a crystallization peak at 58 °C and has a crystallization enthalpy of 149 J g^{-1}, whereas the PS:wax microcapsules crystallize at 53 °C with a crystallization enthalpy of 40 J g^{-1}. These results indicate that the microcapsules contained about 27% wax, which is in line with the observations from the DSC melting results.

The DSC curves of the PP/(PS:wax) and PP/(PS:wax)/SEBS blends are shown in Figures 4.11 and 4.12. The melting temperature of PP is around 165-170 °C. Its melting enthalpy is 83 J g^{-1}. In the case of PP/(PS:wax) and PP/(PS:wax)/SEBS blends, there are two separate endothermic peaks that are related to the melting peaks of the wax and the PP. The melting peak temperatures of the PP and the wax in the blends are shown in Table 4.2. An increase in PS:wax content resulted in a decrease in the melting peak temperatures of PP for both the modified and the unmodified blends. This is the result of the plasticizing effect of the microcapsules on the PP matrix, and the presence of SEBS does not change this behaviour, probably because SEBS forms thin layers around the microcapsules without changing the interfacial interaction between PP and PS:wax.

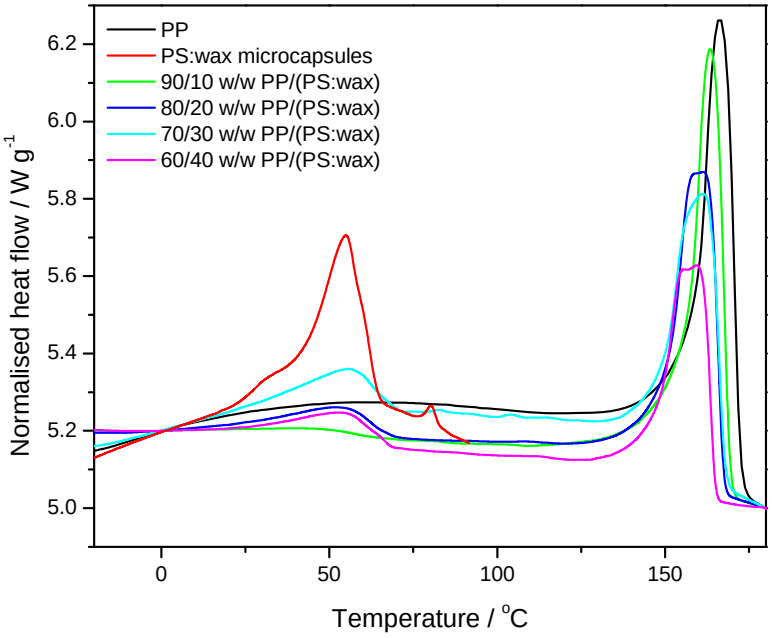

Figure 4.11 DSC curves of PP, PS:wax and the PP/(PS:wax) blends

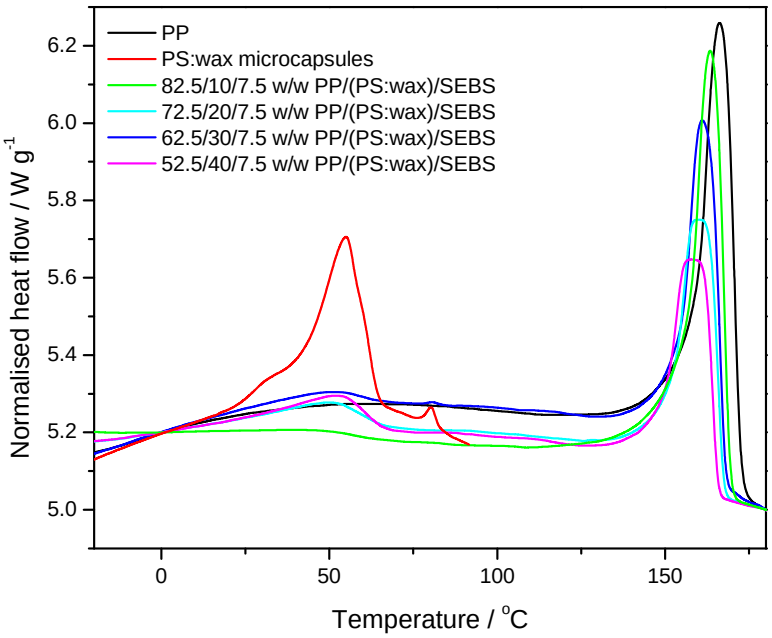

Figure 4.12 DSC curves of PP, PS:wax and the PP/(PS:wax)/SEBS blend

Figures 4.13 shows the experimentally observed and calculated melting enthalpies of PP for the modified and unmodified blends as a function of PS:wax content. When the measured melting enthalpy values (ΔH_m^{obs}) are compared with the calculated values (ΔH_m^{calc}), it can be

seen that the PP in the blends had observably lower melting enthalpy values. It is clear that the PS:wax microcapsules reduced the PP chain mobility which gave rise to a lower crystallinity in both the unmodified and modified systems. This effect was more pronounced in the SEBS modified samples, and the reason for this is not very clear. Most of the results obtained from other techniques indicate that the presence of SEBS did not really change the interfacial interaction between PP and PS:wax. The melting enthalpy results presented in Table 4.2, however, indicate that there may be a slightly enhanced interaction in the presence of SEBS. The standard deviations in both the unmodified and modified blends are small, indicating that the samples were fairly homogenous.

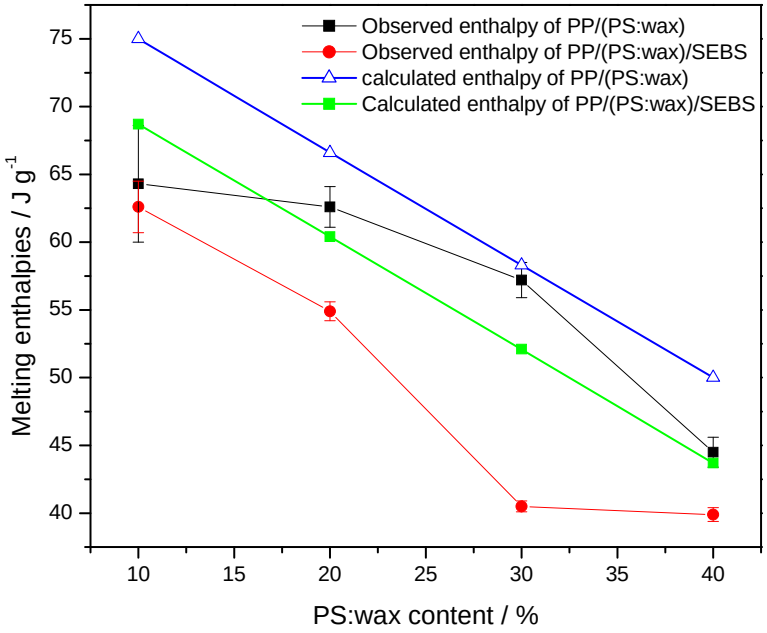

Figure 4.13 Comparison of melting enthalpies of PP/(PS:wax) and PP/(PS:wax)/SEBS blends as a function of PS:wax content

The DSC cooling curves of PP/(PS:wax) and PP/(PS:wax)/SEBS are shown in Figure 4.14 and 4.15. The cooling curves of the blends depict two exothermic peaks, related to the crystallization of PP and of wax. The crystallization peak of PP also shifted to lower temperatures with an increase in the PS:wax microcapsules content. This is in line with the melting data for these samples, and confirms the plasticizing effect of the microcapsules.

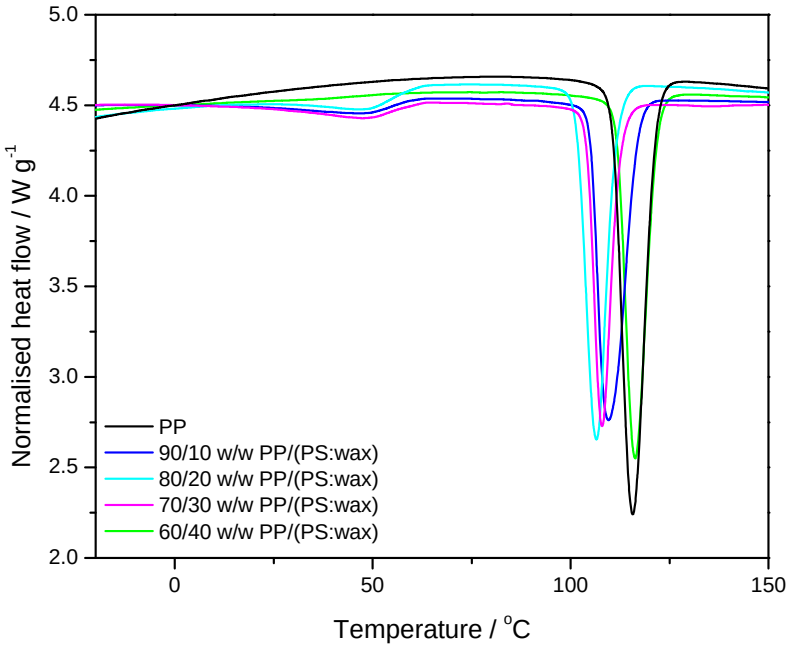

Figure 4.14 DSC cooling curves of PP, PS:wax and the PP/(PS:wax) blends

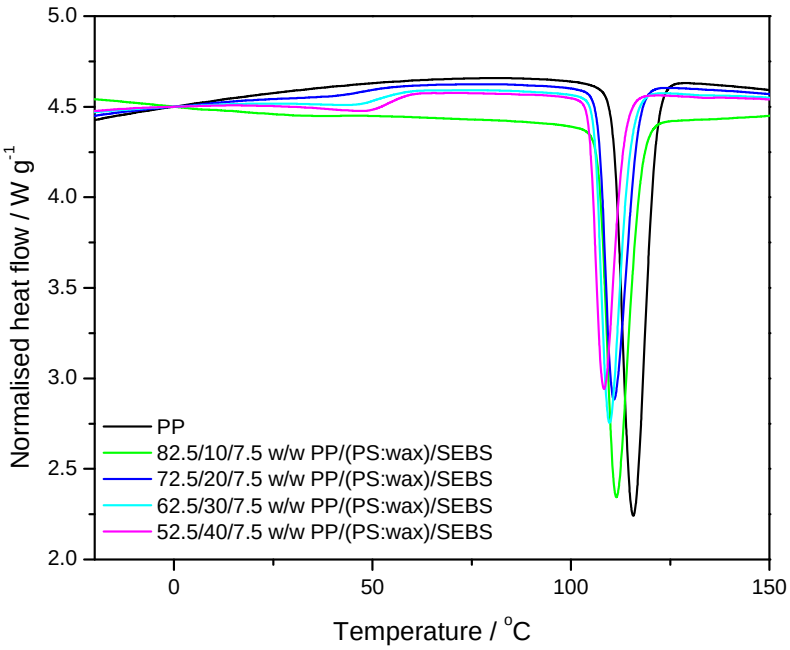

Figure 4.15 DSC cooling curves of PP, PS:wax and the PP/(PS:wax)/SEBS blends

4.5 Dynamic mechanical analysis (DMA)

The dynamic mechanical behaviour of all the samples is shown in Figures 4.16 to 4.27. As can be seen from the storage modulus versus temperature curves in Figure 4.16, there is a drop in storage modulus with increasing PS:wax microcapsules content. There are two possible reasons for this observation. Firstly, it seems as if the microcapsules act as a plasticizer and thus enhances the mobility of the polymer chains, leading to a lower modulus of the polymeric matrix. Samuel *et al.* [8] investigated the viscoelastic properties and glass transition behaviour of bioresorbable poly(lactide-co-glycolide) (PLGA) matrix nanocomposites. They observed that at the physiological temperature of approximately 37 °C the storage modulus of the nanocomposites decreased with nano-particle (α-tricalcium phosphate) loading, and they also explained it as being due to the plasticizing effect of the nano-particles. Secondly, the decreased crystallinity of the blends containing PS:wax microcapsules, as seen from the DSC results (section 4.4), may have contributed to the decrease in storage modulus. It is well-know that the modulus of semi-crystalline polymers is directly related to the crystallinity of these polymers [9-12].

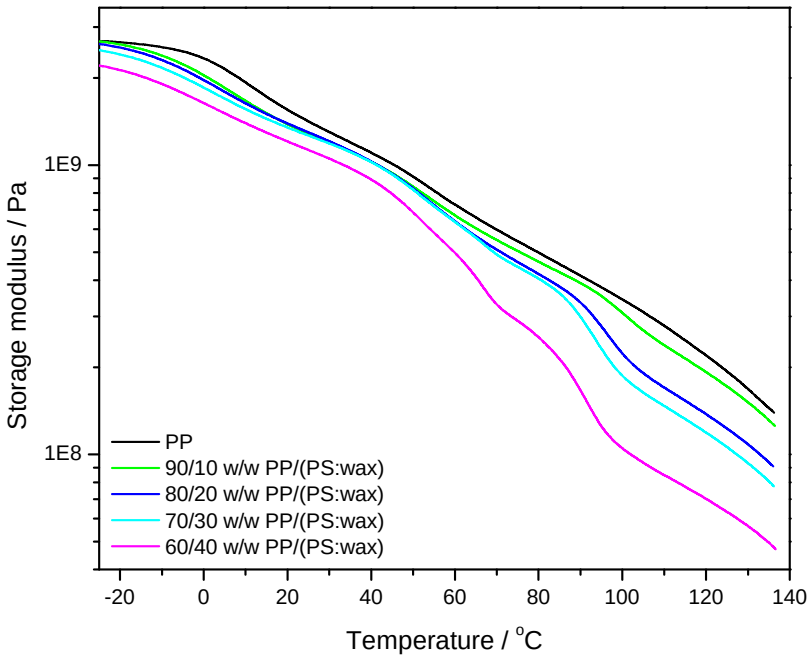

Figure 4.16 DMA storage modulus curves for PP and the PP/(PS:wax) blends

The storage modulus as function of temperature for the PP/(PS:wax)/SEBS blends is shown in Figure 4.17. SEBS had very little effect on the storage modulus of the PP/(PS:wax) blends. SEBS probably forms a thin layer around the microcapsules without improving the interaction between the two phases, and hence SEBS does not change the plasticizing or reinforcing effect of the microcapsules.

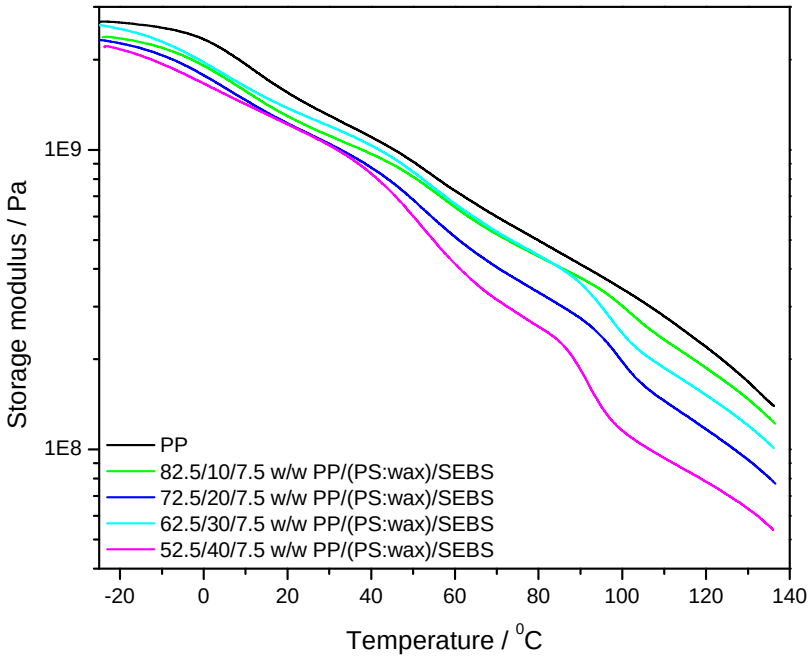

Figure 4.17 DMA storage modulus curves for PP and the PP/(PS:wax)/SEBS blends

The loss modulus and tan δ as a function of temperature for the PP/(PS:wax) and PP/(PS:wax)/SEBS blends are shown in Figures 4.18 to 4.21. The blends exhibit three relaxations. The relaxation between -20 and 30 °C, which is a β relaxation, is attributed to the glass transition of the amorphous phase of PP. Pentti and colleagues [13] reported on the dynamic mechanical properties and morphology of polypropylene/maleated polypropylene blends. They also observed a transition between -20 and 30 °C, which was attributed to the glass transition of PP. The relaxation that occurs at 80-110 °C corresponds to the glass transition of the PS. The transition that occurs between 40 and 60 °C is probably the melting of the wax, and it is more obvious in the loss modulus curves (Figures 4.18 and 4.19). As the PS:wax microcapsules content in the blends increases, the peak intensity of the PS glass transition increases, and this is more obvious in the tan δ plots (Figures 4..20 and 4.21). An increase in the PS:wax microcapsules content also shifts the glass transition of PS to lower

temperatures (Figure 4.20). This may be attributed to an increase in the mobility of the PS chains above the melting point of the wax, with the molten wax acting as a plasticizer. The glass transition of PP in the blends moved to lower temperatures when compared to that of pure PP. This may be attributed to the plasticizing effect of the microcapsules in the blends, as discussed earlier in this section. It does not seem as if the blends behaved any differently in the presence of SEBS, because, as already discussed above, the SEBS probably forms a thin layer around the microcapsules without affecting the interaction between PP and the microcapsules.

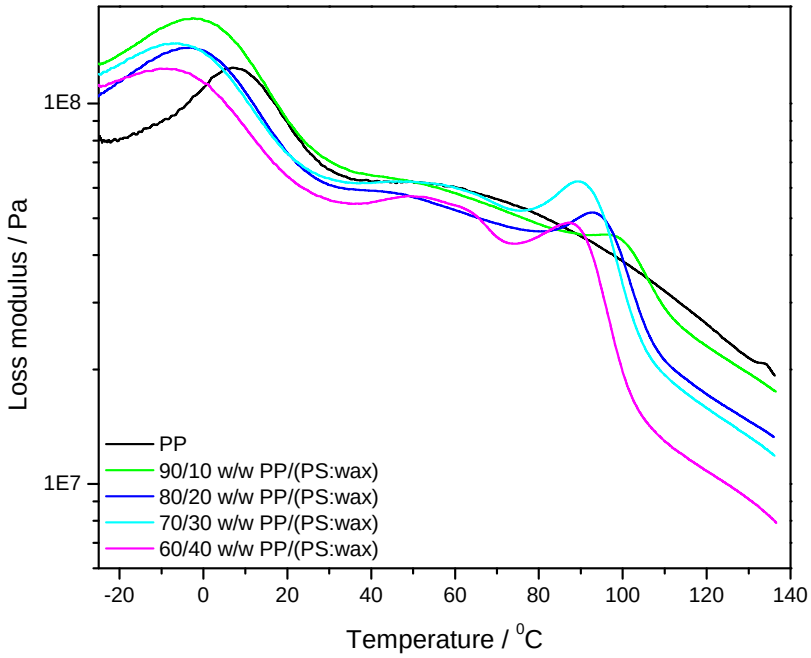

Figure 4.18 DMA loss modulus curves for PP and the PP/(PS:wax) blends

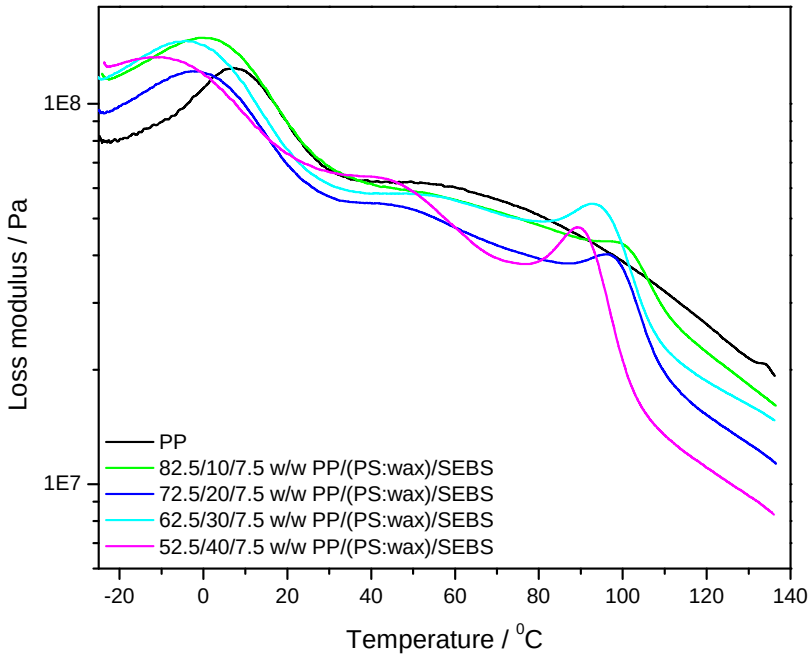

Figure 4.19 DMA loss modulus curves for PP and the PP/(PS:wax)/SEBS blends

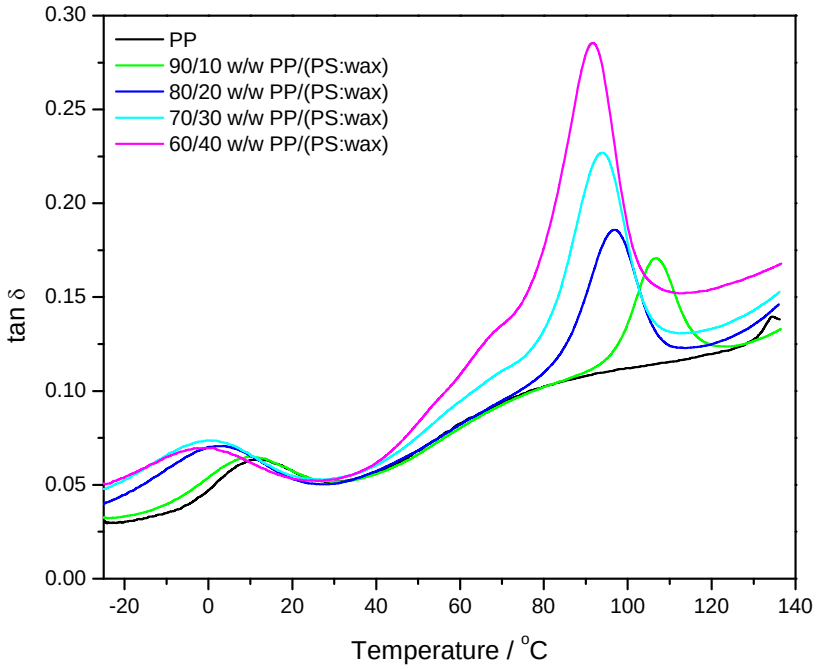

Figure 4.20 DMA tan δ curves for PP and the PP/(PS:wax) blends

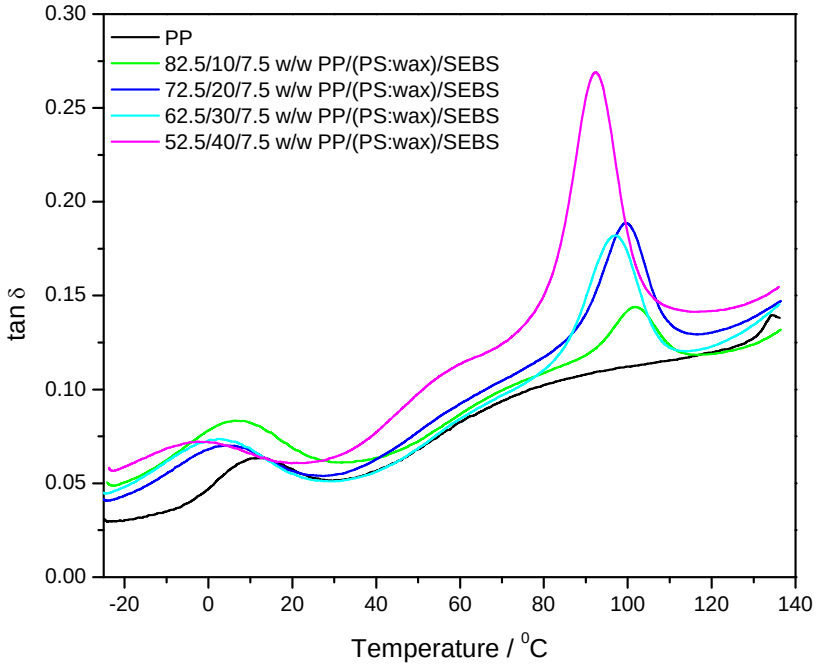

Figure 4.21 DMA tan δ curves for PP and the PP/(PS:wax)/SEBS blends

The storage modulus as a function of temperature of the PP/PS and PP/PS/SEBS blends are shown in Figures 4.22 and 4.23. Generally the storage modulus of the blends, in the absence and presence of SEBS, are higher than that of unblended PP below the glass transition of PS. However, above the glass transition of PS the storage modulus for both PP/PS and PP/PS/SEBS decreases to values below that of PP. The modulus reduction at the PS glass transition also becomes more significant with increasing PS content, as expected. This may be attributed to the higher flexibility of the PS chains above its glass transition. It does not seem as if the blends behaved any differently in the presence of SEBS. In this case the SEBS is probably also located at the interface of the PP and PS phases, and it probably does not change the interaction between these phases.

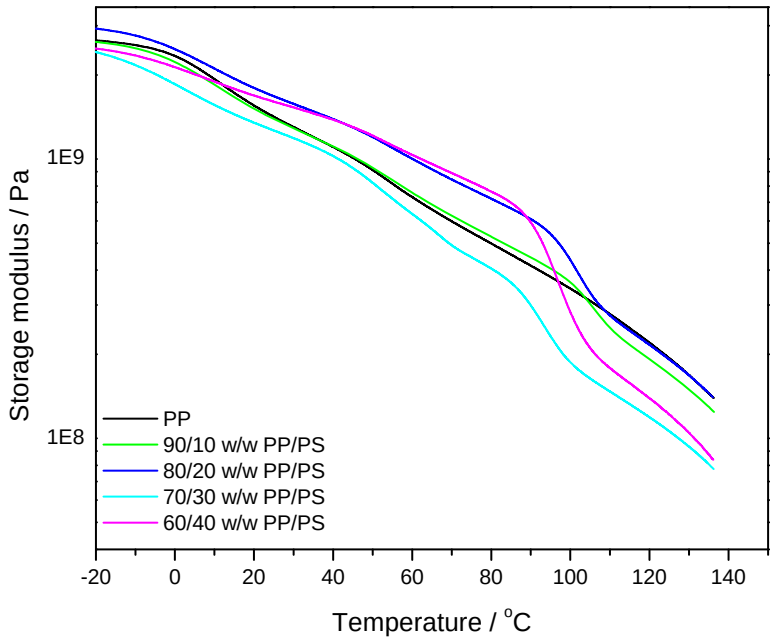

Figure 4.22 DMA storage modulus curves for the PP/PS blends

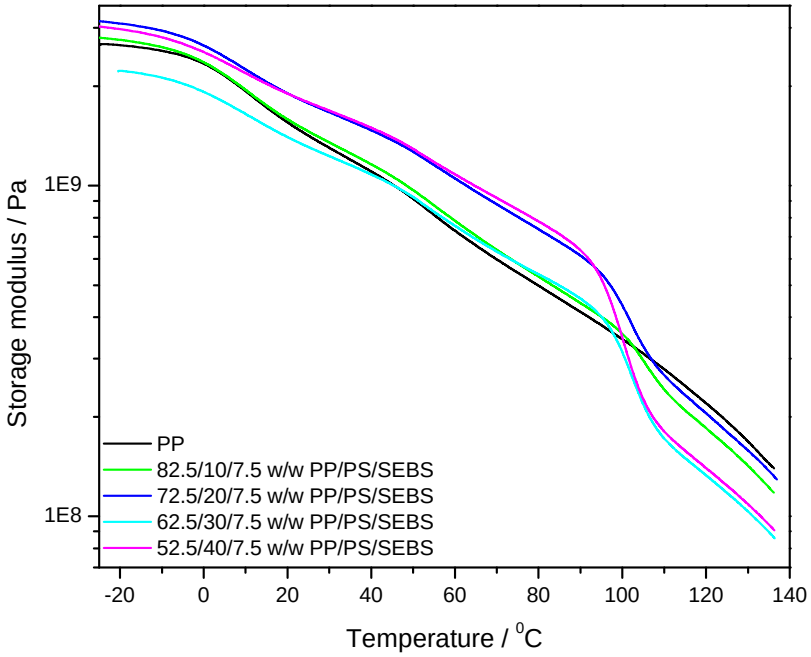

Figure 4.23 DMA storage modulus curves for PP/PS/SEBS blends

The loss modulus and tan δ curves of the modified and unmodified PP/PS blends are shown in Figures 4.24 to 4.27. It is noticed that an increase in the PS content in the PP/PS and PP/PS/SEBS blends increased the peak height corresponding to the PS glass transition in both the loss modulus and tan δ plots. This means that the magnitude of the peak is related to the PS content in the blends. It is worth noting that in both the loss modulus and tan δ curves of the PP/PS blends the glass transition temperature of the PP remains unchanged when compared to that of pure PP. The shift in glass transition is not expected as such variations are normally observed in partially or fully miscible blends where (partial) miscibility generates a variation in T_g with composition [14]. However, in the blends with PS:wax microcapsules the glass transition of PP shifted to lower temperatures when compared to that of the pure PP (Figures 4.18 to 4.21), which confirms the plasticizing effect of the microcapsules.

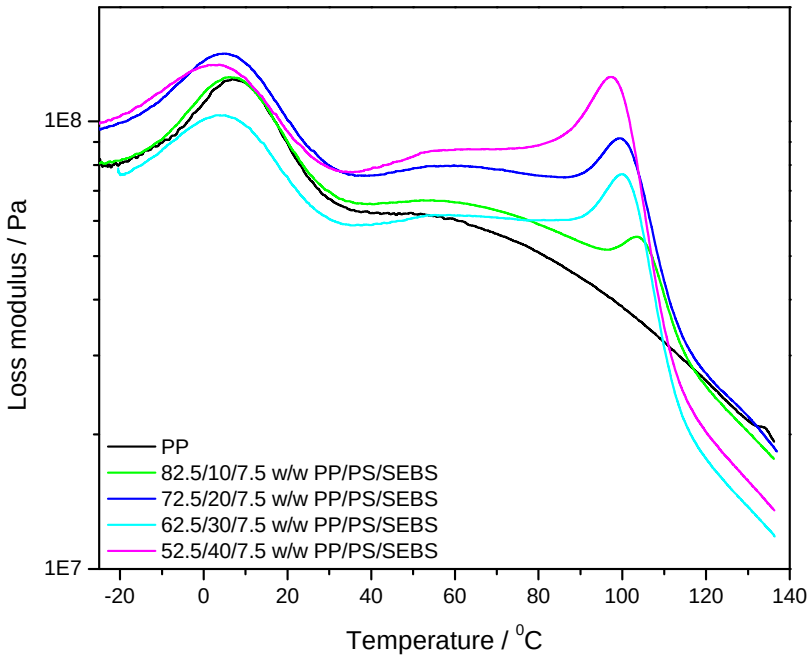

Figure 4.24 DMA loss modulus curves for PP and the PP/PS/SEBS blends

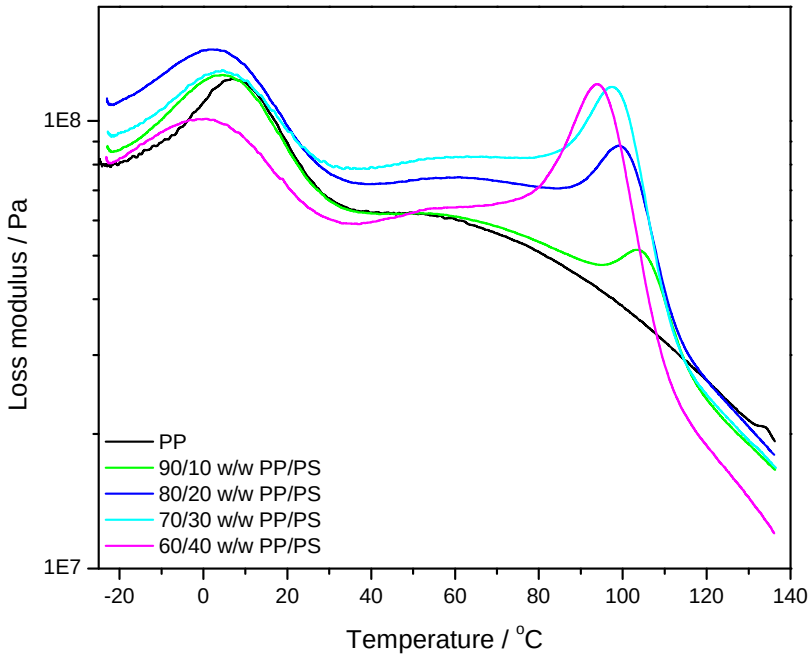

Figure 4.25 DMA loss modulus curves for PP and the PP/PS blends

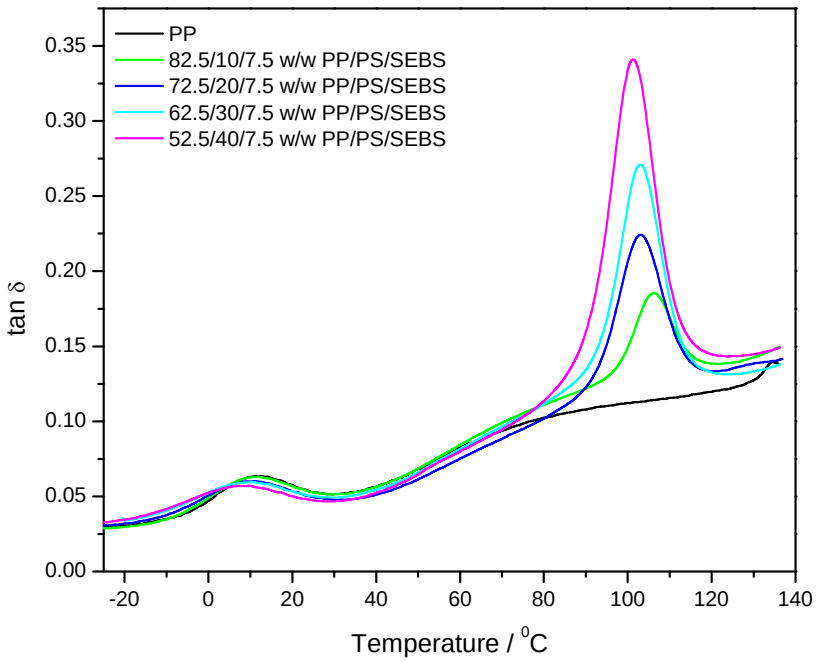

Figure 4.26 DMA tan δ curves for PP and the PP/PS/SEBS blends

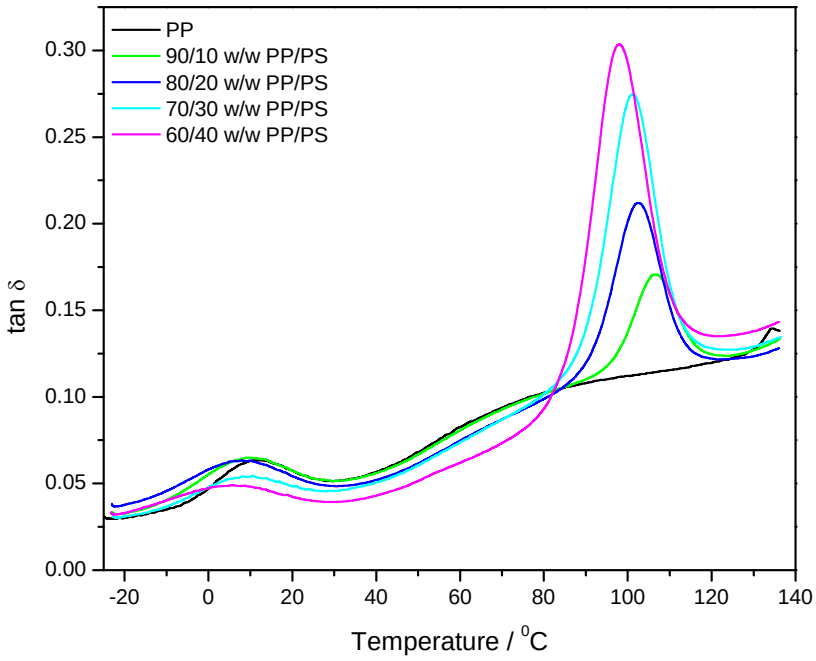

Figure 4.27 DMA tan δ curves for PP and the PP/PS/SEBS blends

4.6 Tensile testing

The tensile properties of all the investigated samples are depicted in Figures 4.28 to 4.37. The actual values of these properties are summarized in Tables 4.3 and 4.4. All the stress-strain curves are presented in the Appendix. The stress at break of the PP/(PS:wax) and PP/PS blends (Figure 4.28 to 4.29) decreases with increasing PS:wax and PS contents. The reasons that the PS:wax and PS gives low stress at break is related to the weak interfacial interaction between PP and PS, so that the interfaces between the non-compatible polymers act as defects points where stress cracking will occur more easily. The presence of SEBS does not change this behaviour, probably because SEBS forms thin layers around the microcapsules without changing the interfacial interaction between PP and PS.

Table 4.3 Summary of tensile results for PP/(PS:wax) blends and PP/(PS:wax)/SEBS blends

Sample	σ_b / MPa	ε_y / %	ε_b / %	σ_y / MPa	E / MPa
PP/(PS:wax)					
100/0	29.5 ± 3.2	12.4 ± 1.0	16.7 ± 1.2	36.3 ± 0.4	756 ± 25
90/10	27.5 ± 3.1	9.2 ± 1.6	12.5 ± 2.0	28.9 ± 2.8	742 ± 105
80/20	20.9 ± 0.9	7.2 ± 1.0	10.6 ± 1.3	21.8± 1.5	752 ± 46
70/30	15.3 ± 1.5	5.4 ± 1.2	5.8 ± 1.4	15.5 ± 1.6	715 ± 43
60/40	11.5 ± 1.2	3.9 ± 0.7	4.9 ± 1.8.	11.6 ± 1.2	760 ± 67
PP/(PS:wax) /SEBS					
82.5/10/7.5	22.1± 1.6	9.3 ± 0.6	22.2 ± 6.6	26.1 ± 0.5	729 ± 46
72.5/20/7.5	22.0 ± 1.6	8.3 ± 0.8	19.3 ± 2.4	24.1 ± 1.5	666 ± 46
62.5/30/7.5	17.6 ± 1.2	6.5 ± 0.4	12.8 ± 1.0	16.8 ± 0.9	516 ± 26
52.5/40/7.5	16.6 ± 0.9	6.4 ± 0.4	7.0 ± 0.7	16.7 ± 0.9	610 ± 46

ε_y, σ_y, ε_b, σ_b and E are elongation at yield, yield stress, elongation at break, stress at break, and Young's modulus of elasticity.

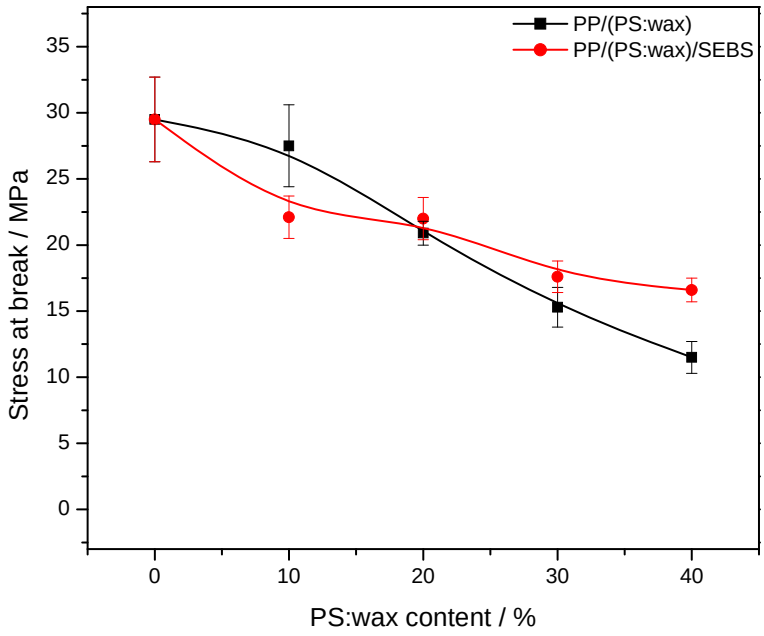

Figure 4.28 Stress at break of PP/(PS:wax) and PP/(PS:wax)/SEBS blends as function of PS:wax content

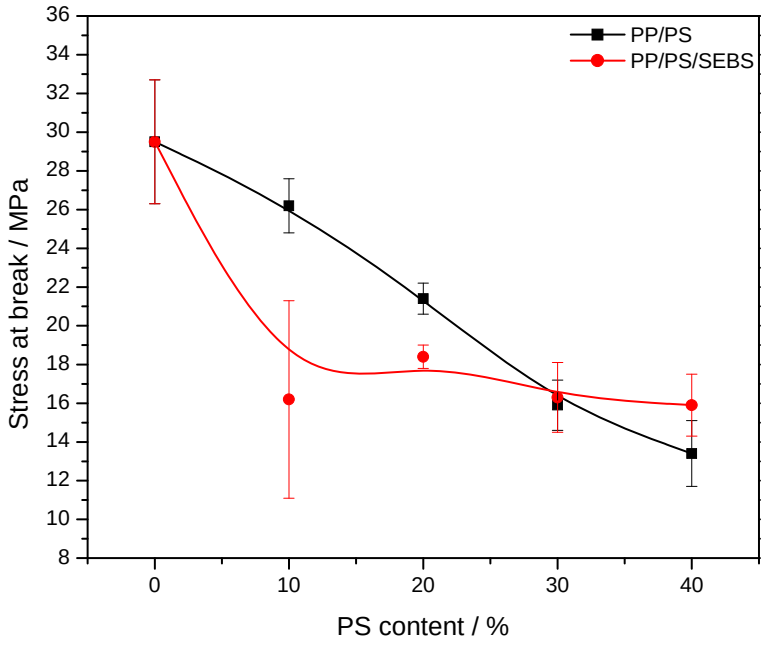

Figure 4.29 Stress at break of PP/PS and PP/PS/SEBS blends as function of PS content

An increase in PS:wax content resulted in a decrease in elongation at break for the investigated PP/(PS:wax) blends (Figure 4.30). This can be explained by the PS:wax microcapsules acting as defect points for the initiation and propagation of stress cracking. The blends with SEBS (Figure 4.31) show significantly higher elongation at break values than the unmodified blends. This effect may be ascribed to the more mobile SEBS layer which reduced the stiffening effect of the blends and increased their flexibility. The elongation at break for the PP/PS:wax/SEBS blends at PS:wax contents of 10 and 20 wt % is higher than that of neat PP, but decreases to values below that of neat PP with a further increase in PS:wax content. This may be attributed to the effective covering of the microcapsules when their content was low (the SEBS content was constant at 7.5 wt.%), but ineffective covering at higher microcapsule contents. The PP/PS and PP/PS/SEBS blends (Figure 4.31) showed similar behaviour and can be explained in the same way.

Table 4.4 Summary of tensile results for PP/PS blends and PP/PS/SEBS blends

Sample	σ_b / MPa	ε_y / %	ε_b / %	σ_y / MPa	E / MPa
PP/PS					
100/0	29.5 ± 3.2	12.4 ± 1.0	16.7 ± 1.2	36.3 ± 0.4	756 ± 25
90/10	26.2 ± 1.4	7.3 ± 0.4	16.1 ± 3.8	28.1 ± 1.6	883 ± 71
80/20	21.4 ± 0.8	5.7 ± 0.7	17.4 ± 3.6	23.9 ± 0.8	930 ± 24
70/30	15.9 ± 1.3	5.4 ± 2.3	12.8 ± 1.0	18.2 ± 0.3	931 ± 13
60/40	13.4 ± 1.7	5.2 ± 1.8	15.7 ± 3.2	13.4 ± 1.7	944 ± 92
PP/PS/SEBS					
82.5/10/7.5	16.2 ± 5.1	7.8 ± 0.4	44.9 ± 15.0	25.6 ± 0.5	766 ± 25
72.5/20/7.5	18.4 ± 0.6	7.6 ± 1.9	21.7 ± 5.2	20.6 ± 0.3	797 ± 71
62.5/30/7.5	16.3 ± 1.8	6.9 ± 1.3	11.3 ± 2.3	19.7 ± 0.5	750 ± 24
52.5/40/7.5	15.9 ± 1.6	6.2 ± 1.1	7.7 ± 0.8	17.3 ± 1.1	779 ± 13

ε_y, σ_y, ε_b, σ_b and E are elongation at yield, yield stress, elongation at break, stress at break, and Young's modulus of elasticity.

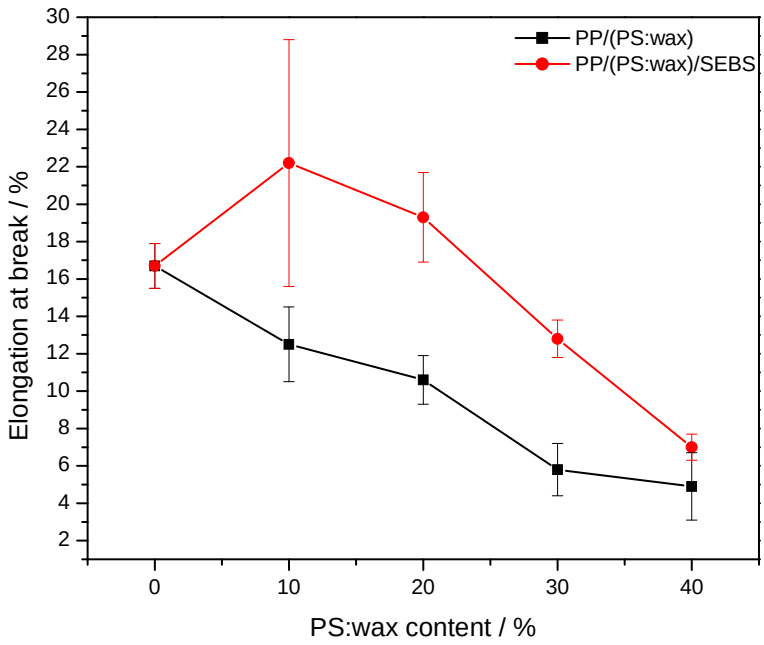

Figure 4.30 Elongation at break of PP/(PS:wax) and PP/(PS:wax)/SEBS blends as function of PS:wax content

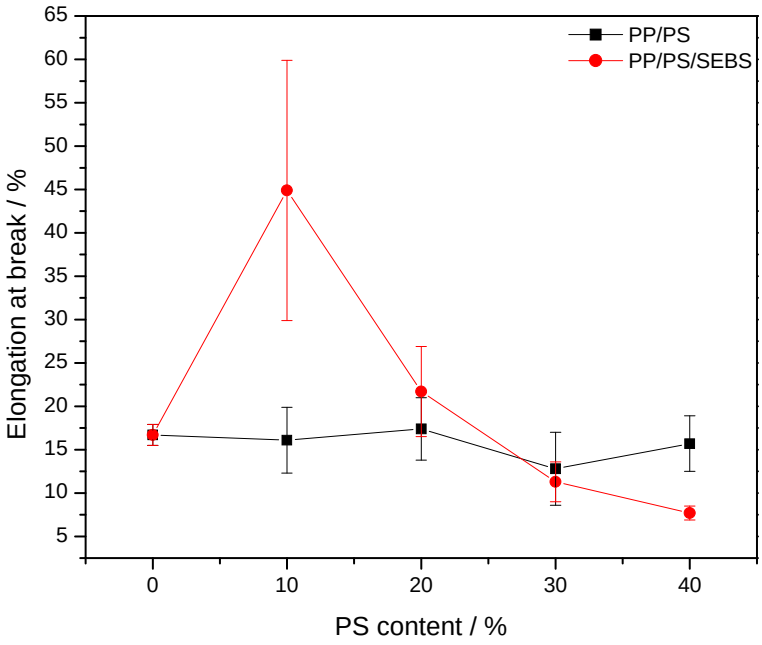

Figure 4.31 Elongation at break of PP/PS and PP/PS/SEBS blends as function of PS content

The stress and elongation at yield for all the PS:wax and PS containing samples are shown in Figures 4.32 to 4.35. Elongation at yield of neat PP depends on the strengthening of tie molecules as intercrystalline and interspherulitic links in the amorphous layers [18]. The incorporation of PS:wax or PS into PP decreased the elongation at yield (Figures 4.32 and 4.33), which can be ascribed to the dispersed PS:wax or PS increasing the rigidity of the blend and making it less ductile. The PP/PS/SEBS and PP/(PS:wax)/SEBS blends show slightly higher elongation at yield values over the whole composition range when compared to PP/PS and PP/(PS:wax) blends; this is due to the addition of SEBS which is an elastomer that provides more flexibility which results in higher elongations. Similar results were obtained by Denac *et al.* [19], who studied PP/talc/SEBS (SEBS-g-MA) composites. They observed that the addition of talc reduced the elongation at yield, but that the incorporation of SEBS improved the elongation at yield. The yield stress decreased with increasing PS:wax content for both the unmodified and modified blends (Figures 4.34 and 4.35). This decrease is associated with the decrease in the crystallinity of the blends, since yield stress is a function of crystallinity.

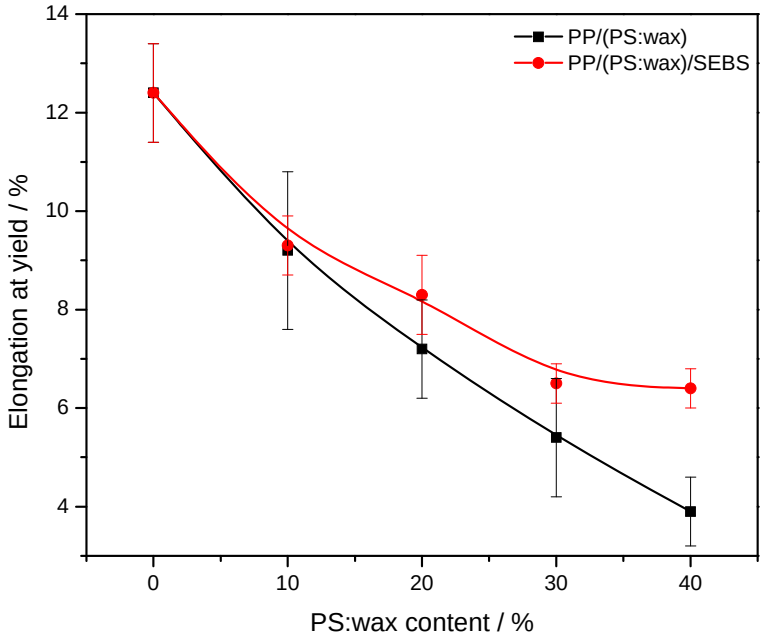

Figure 4.32 Elongation at yield of PP/(PS:wax) and PP/(PS:wax)/SEBS blends as function of PS:wax content

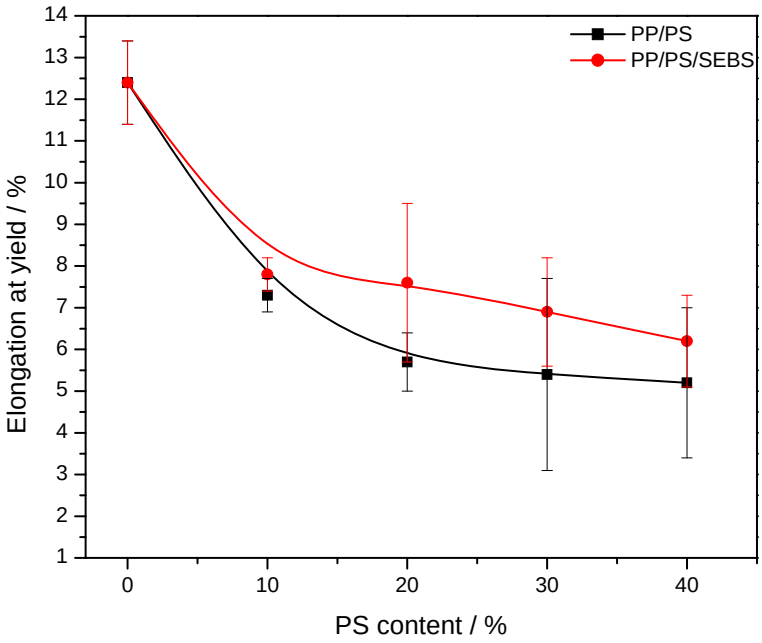

Figure 4.33 Elongation at yield of PP/PS and PP/PS/SEBS blends as function of PS content

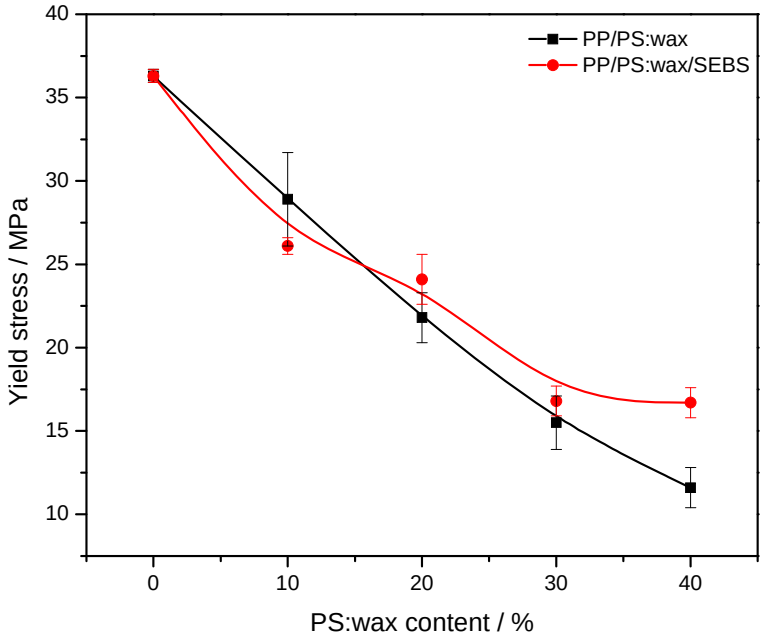

Figure 4.34 Yield stress of PP/(PS:wax) and PP/(PS:wax)/SEBS blends as function of PS:wax content

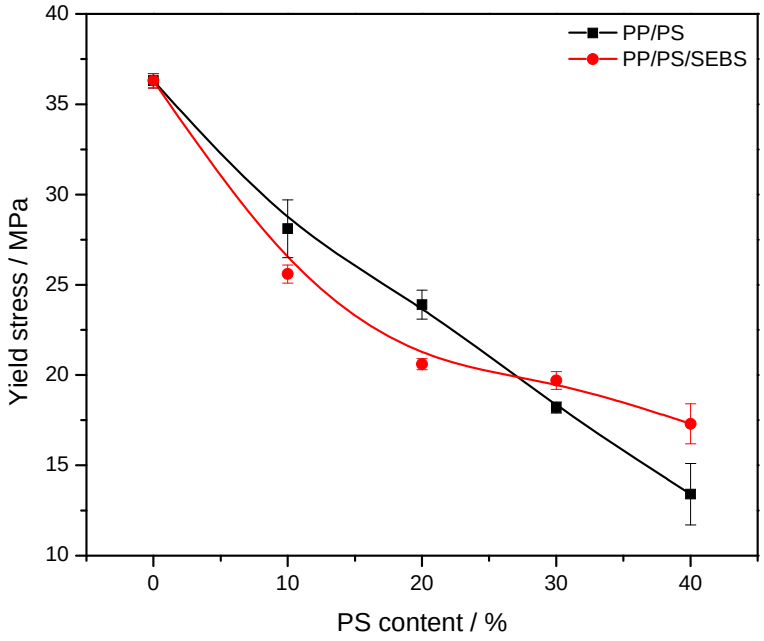

Figure 4.35 Yield stress of PP/PS and PP/PS/SEBS blends as function of PS content

Figures 4.36 and 4.37 show the Young's modulus of the modified and unmodified PP/(PS:wax) and PP/PS blends. Young's modulus of the unmodified blends is higher than those of the modified blends for all the PS:wax and PS contents. There are three possible reasons for this behaviour. The first is the higher crystallinity of the unmodified blends. Secondly, it seems as if SEBS acts as a lubricant which creates more free volume and improves the mobility of the polymer chains, especially at the PP-PS:wax and PP-PS interface, and hence reduces the stiffness of the blends. A similar observation was reported by Leu *et al*. [20] who investigated the morphology, as well as the mechanical and thermal properties, of injection molded poly(lactic acid)/SEBS-g-MAH/organomontmorillonite nanocomposites. They associated the decrease in modulus with the elastomeric nature of SEBS-g-MAH. Thirdly, the higher modulus of the unmodified blends is the result of the addition of a rigid polymer (PS) into the PP matrix. It is noticed that the modulus of PP/PS:wax does not change with increasing PS:wax content in the absence of SEBS (Figure 4.36), while the modulus decreases with increasing PS:wax content in the presence of SEBS. However, for PP/PS (Figure 4.37) the modulus increases with increasing PS content for the unmodified blends while there is almost no change for the blends prepared in the presence of SEBS. The reason for this is not clear, but it must be related to the differences in morphology between the PP/PS:wax and the PP/PS.

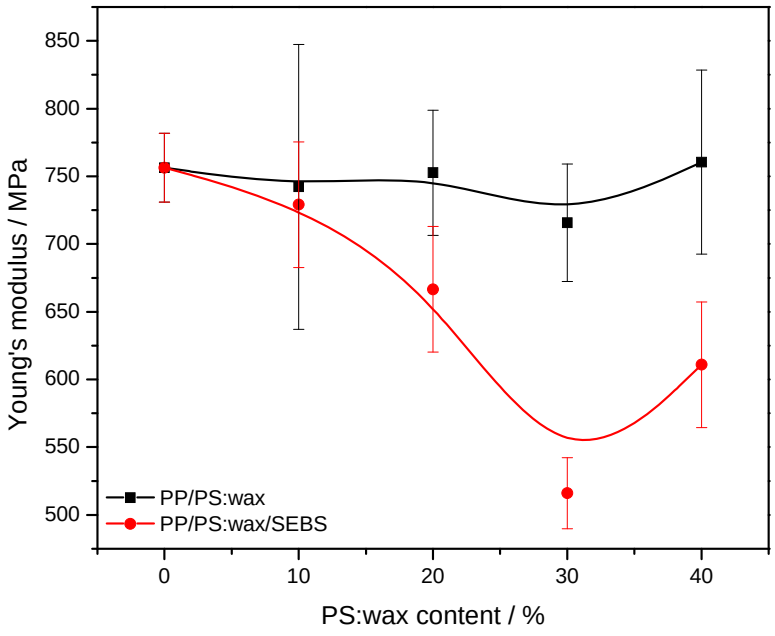

Figure 4.36 Young's modulus of PP/(PS:wax) and PP/(PS:wax)/SEBS blends as function of PS:wax content

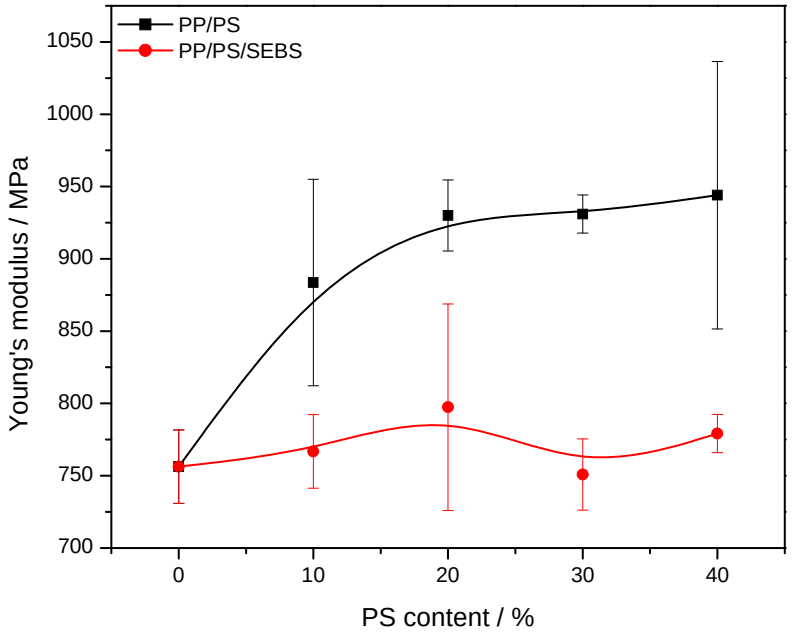

Figure 4.37 Young's modulus of PP/PS and PP/PS/SEBS blends as function of PS content

4.7 Thermal conductivity

The thermal conductivities of the paraffin, PP/PS:wax and PP/PS:wax/SEBS blends were measured at room temperature using a thermal conductivity apparatus, and the results are shown in Table 4.5 and Figure 4.38. The thermal conductivity of the wax in the solid state is 0.20 W m^{-1} K^{-1}, that of PP is 0.22 W m^{-1} K^{-1}, and that of PS is 0.03 W m^{-1} K^{-1}.

The thermal conductivities of the unmodified and modified blends decrease with increasing PS:wax microcapsule content in the blends. The polystyrene shell has a much lower conductivity than the PP matrix, which explains the lower thermal conductivities of the blends with increasing PS content. The thermal conductivities of the unmodified blends are slightly higher than those of the modified blends, even though the difference is not significant. SEBS has a very low thermal conductivity [21]; hence it may have contributed to the lower thermal conductivities of the modified blends.

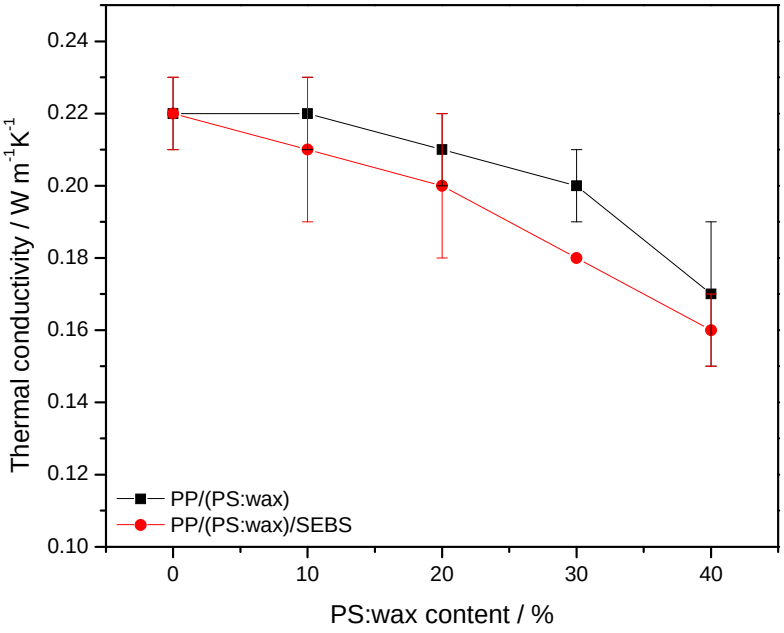

Figure 4.38 Thermal conductivity of modified and unmodified blends as a function of PS:wax content

Table 4.5 Thermal conductivity measurements of investigated blends

Sample (w/w)	Thermal conductivity / W m^{-1} K^{-1}
PP/(PS:wax)	
90/10	0.22 ± 0.01
80/20	0.21 ± 0.01
70/30	0.20 ± 0.02
60/40	0.17 ± 0.02
PP/(PS:wax)/SEBS	
82.5/10/7.5	0.21 ± 0.02
72.5/20/7.5	0.20 ± 0.02
62.5/30/7.5	0.18 ± 0.00
52.5/40/7.5	0.16 ± 0.01

4.8 References

1. N. Sarier, E. Onder. The manufacture of microencapsulated phase change materials suitable for design of thermally enhanced fabrics. Thermochimica Acta 2007; 452:149-160.
   DOI:10.1016/j.tca.2006.08.002
2. G. Fang, H. Li, F. Yang, X. Liu, S. Wu. Preparation and characterization of nano-encapsulated n-tetradecane as phase change material for thermal energy storage. Chemical Engineering Journal 2009; 153:217-221
   DOI:10.1016/j.cej.2009.06.019
3. L. Sánchez-Silva, J.F. Rodríguez, A. Romero, A.M. Borreguero, M. Carmona, P. Sánchez. Microencapsulation of PCMs with a styrene-methyl methacrylate copolymer shell by suspension-like polymerisation. Chemical Engineering Journal 2010; 157:216-222.
   DOI:10.1016/j.cej.2009.12.013
4. A.M. Borreguero, J.L. Valverde, J.F. Rodríguez, A.H. Barber, J.J. Cubillo, M. Carmona. Synthesis and characterization of microcapsules containing Rubitherm®RT27 obtained by spray drying. Chemical Engineering Journal 2011; 166:384-390.
   DOI:10.1016/j.cej.2010.10.055
5. J. Li, P. Xue, W. Ding, J. Han, G. Sun. Micro-encapsulated paraffin/high-density polyethylene/wood flour composite as form-stable phase change material for thermal storage. Solar Energy Materials and Solar Cells 2009; 93:1761-1767
   DOI:10.1016/j.solmat.2009.06.007
6. H.H. Ismail, M. Nasir. Morphological studies of uncompatibilized and compatibilized polystyrene/polypropylene blend. Polymer Testing 2002; 21:263-267.
   DOI:10.1016/S0142-9418(01)00079-4
7. L. Sánchez, P. Sánchez, A. de Lucas, M. Carmona, J.F. Rodriguez. Microencapsulation of PCMs with a polystyrene shell. Colloid and Polymer Science 2007; 285:1377-1385.
   DOI:10.1007/s00396-007-1696-7
8. I. Samuel, J. Wilberforce, S.M. Best. A dynamic mechanical thermal analysis study of the viscoelastic properties and glass transition temperature behaviour of bioresorbable polymer matrix nanocomposites. J Material Sci: Mater Med 2010; 21:3085-3093

DOI:10.1007/s10856-010-4170-x

9. C. Komalan, K.E. George, P.A.S Kumar, K.T. Varughese, S. Thomas. Dynamic mechanical analysis of binary and ternary polymer blends based on nylon copolymer/EPDM rubber and EPM grafted maleic anhydride compatibilizer. eXPRESS Polymer Letters 2007;10:641-653.
DOI:10.3144/expresspolymlett.2007.88
10. W. Herrera-Kao, M. Aguilar-Vega. Storage modulus changes with temperature in poly(vinyl alcohol), PVA, /poly(acrylic acid), PAA, blends. Polymer Bulletin 1999; 42:449-456
11. E.S. Kumar, C.K. Das. Mechanical, dynamic mechanical properties and thermal stability of fluorocarbon elastomer-liquid crystalline polymer blends. Polymer Composites 2005; 26:306-315.
DOI:10.1002/pc.20102
12. A. Sedighiamiri, T.B. Van Erp, G.W.M. Peters, L.E. Govaert, J.A.W. Van Dommelen. Micromechanical modeling of the elastic properties of semicrystalline polymers: A three-phase approach. Journal of Polymer Science: Part B: Polymer Physics 2010; 48:2173-2184.
DOI:10.1002/polb.22099
13. J. Pentti, L. Shucai, P. Järvela. Dynamic mechanical properties and morphology of polypropylene/maleated polypropylene blends. Journal of Applied Polymer Science 1996; 62:813-826.
DOI:10.1002/(SICI)1097-4628(19961031)
14. V. Thirtha, R. Lehman, T. Nosker. Glass transition phenomena in melt-processed polystyrene/ polypropylene blends. Polymer Engineering and Science 2005; 45:1187-1193.
DOI:10.1002/pen.20387
15. I. Krupa, G. Miková, A.S. Luyt. Polypropylene as a potential matrix for the creation of shape stabilized phase change materials. European Polymer Journal 2007; 43:895-907.
DOI:10.1016/j.eurpolym.2006.12.019
16. I. Krupa, G. Miková, A.S. Luyt. Phase change materials based on low-density polyethylene/paraffin wax blends. European Polymer Journal 2007; 43:4695-4705.
DOI:10.1016/j.eurpolymj.2007.08.022

17. A. Sari, C. Alkan, A. Karaipeki. Preparation, characterization and thermal properties of PMMA/n-heptadecane microcapsules as novel solid-liquid microPCM for thermal energy storage. Applied Energy 2010; 87:1529-1534
DOI:10.1016/j.apenergy.2009.10.011

18. I. Švab, V. Musil, I. Šmit, M. Makarovic. Mechanical properties of wollastonite-reinforced polypropylene composites modified with SEBS and SEBS-g-MA elastomers. Polymer Engineering and Science 2007; 47:1873-1880
DOI:10.1002/pen.20897

19. M. Denac, V. Musil, I. Šmit. Polypropylene/talc/(SEBS-g-MA) composites. Part 2. Mechanical properties. Composites: Part A 2005; 36:1282-1290.
DOI:10.1016/J.compositesa.2005.01.011

20. Y.Y. Leu, Z.A. Mohd Ishak, W.S. Chow. Mechanical, thermal, and morphological properties of injection molded poly(lactic acid)/SEBS-g-MAH/organo-montmorillonite nanocomposites. Journal of Applied Polymer Science (In press)
DOI:10.1002/app.35084

21. D. Juárez, S. Ferrand, O. Fenollar, V. Fombuena, R. Balart. Improvement of thermal inertia of styrene-ethylene/butylene-styrene (SEBS) polymers by addition of microencapsulated phase change materials (PCMs). European Polymer Journal 2011; 47:153-161.
DOI:10.1016/j.eurpolymj.2010.11.004

Chapter 5: Conclusions

The purpose of this study was to investigate (i) the morphology and properties of polypropylene (PP) containing PS encapsulated soft paraffin wax to be used as phase change material for energy storage, and (ii) the effect of SEBS modifier, which is normally used for improved dispersion of fillers in polymers, on the properties of PP/(PS:wax) and PP/PS blends.

Polystyrene microcapsules containing soft paraffin wax were prepared by suspension polymerization. The experimental results show that between 20 and 30 wt% of wax was encapsulated in the PS shell. Based on these results it can be concluded PCM storage capacity was severely reduced by PS encapsulation of the wax, and therefore our investigated system will probably not be an effective PCM.

The presence of PS:wax microcapsules in the PP influenced the morphology and properties of the matrix. Generally a fairly good interaction between the microparticles and the matrix was observed, even in the absence of SEBS. The PS:wax acted as a plasticizer in the PP matrix reducing the thermal stability, storage modulus and melting temperature of the matrix. It was found that the addition of microcapsules decreased the mechanical properties of the blends. The decrease in tensile strength, elongation at break and yield stress is evidence of the deterioration of the mechanical properties. The results also show a decrease in conductivity of the PP/PS:wax blends with the addition of the microcapsules because of the lower thermal conductivity of PS.

The results obtained from most techniques indicate that the presence of SEBS did not really change the interfacial interaction between PP and PS:wax, and probably formed a thin layer around the microcapsules. It can be concluded that SEBS at 7.5 wt% did not really modify the PP/PS:wax PCM system. The presence of SEBS in the blends really only improved the flexibility of the blends. This was evidenced by the decrease in Young's modulus and the elongation at break in the presence of SEBS when compared to the unmodified blends. The results also show that SEBS was effective in covering the microcapsules when their content was low, but ineffective at higher microcapsule contents. The effectiveness of SEBS therefore depends on the blend composition. It was found that the blends with SEBS were

more thermally stable than the unmodified blends. In this case SEBS probably acted as a heat isolator.

Generally there was very little difference between the properties of the PP/PS:wax and the PP/PS systems, except at high contents of the microcapsules and the dispersed PS. In the latter case the differences in morphology (PS:wax microcapsules being spheres in the PP matrix, even at high microcapsule contents, while PS may have started forming a co-continuous blend with PP) may have influenced the different properties.

Recommendations for future work:

- The addition of conductive filler within the encapsulated PCM to enhance the thermal conductivity of the PCM systems.
- In order to improve the storage capacity of the microcapsules, the effect of core/shell mass ratio in the microcapsules has to be improved.

ACKNOWLEDGEMENTS

The preparation of this thesis would not have been possible without the will of the Almighty God and the support, hard work and endless efforts of a large number of individuals and institutions.

I would like to thank my supervisor, **Prof. Adriaan Stephanus Luyt,** for his great efforts to explain things clearly and simply, and his guidance during my research. I express my deep sense of gratitude for his guidance, cloudless source of inspiration and constant support all through the course of the study. Throughout my thesis-writing period, he provided encouragement, sound advice, good teaching, good company, and lots of good ideas. His overly enthusiasm and integral view on research and his mission for providing 'only high-quality work and not less', has made a deep impression on me. I owe him lots of gratitude for having shown me this way of research. He could not even realize how much I have learned from him.

I acknowledge the University of the Free State at large by providing me with an opportunity to study. I am grateful to the Faculty programme secretary, Mrs Marlize Jackson, for her unself-centred service rendered.

The credit must be given to my parents (the late Mr. Samuel Mochane and Mrs Elizabeth Mochane) for raising me with their love, guidance, support, responsibility and a lot of encouragement.

Sense of gratitude to all my fellow polymer science research group and colleagues (Dr. Hei Wei, Dr. Nagi Greesh, Mr. Mohammad Essa Ahmad, Mr. Mfiso Mngomezulu, Mr. Tshwafo Motaung, Ms. Julia Puseletso Mofokeng, Mr. Thabang Hendrica Mokhothu, Mr. Teboho Motsoeneng. Mr. Teboho Mokhena, Ms. Motshabi Sibeko, Mr. Jonas Mochane, Mr. Tladi Mofokeng, Ms. N. Nhlapo, Ms. Zanele Clarke, Mr. Tsietsi Tsotetsi, Mrs Nomampondomise Molefe and Neo Moji), for all their help, support, interest and valuable inputs.

All sense of gratitude to my siblings Elias Mochane, Monyatsi Mochane, Mokgethi Mochane, Ntswaki Mochane, and Nthloro Mochane.

I wish to thank greatly my best friends Él Đeeré Bendiciòn de Søùzä Bénìnhø, Motsope Ben Mofokeng, Teboho Motsoeneng, Caravan Motloung, Essa Ahmad, Lefa Mbuli, Luyanda Noto and Teboho Mokhena for helping me get through the tough times, and for all the good ideas shared.

Appendix A

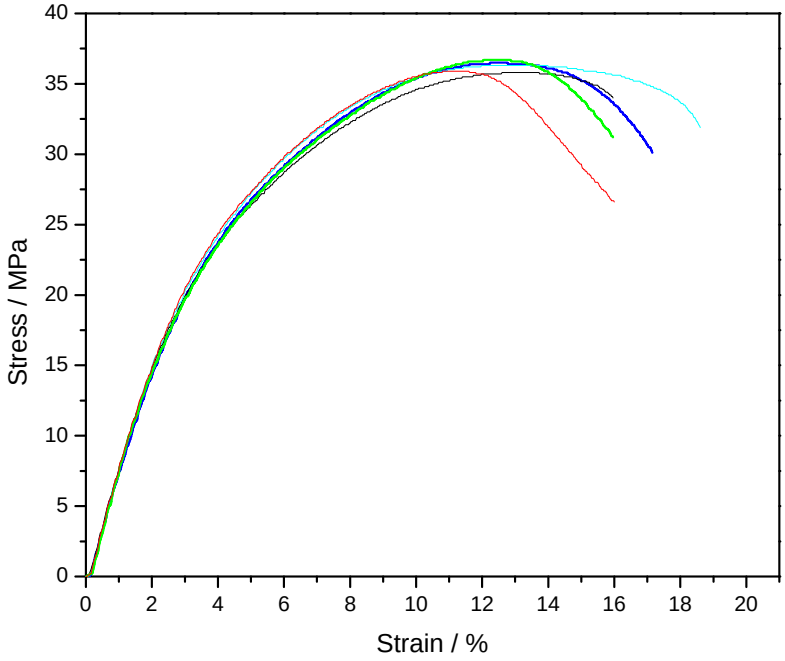

Figure A.1 Stress-strain curves of neat PP

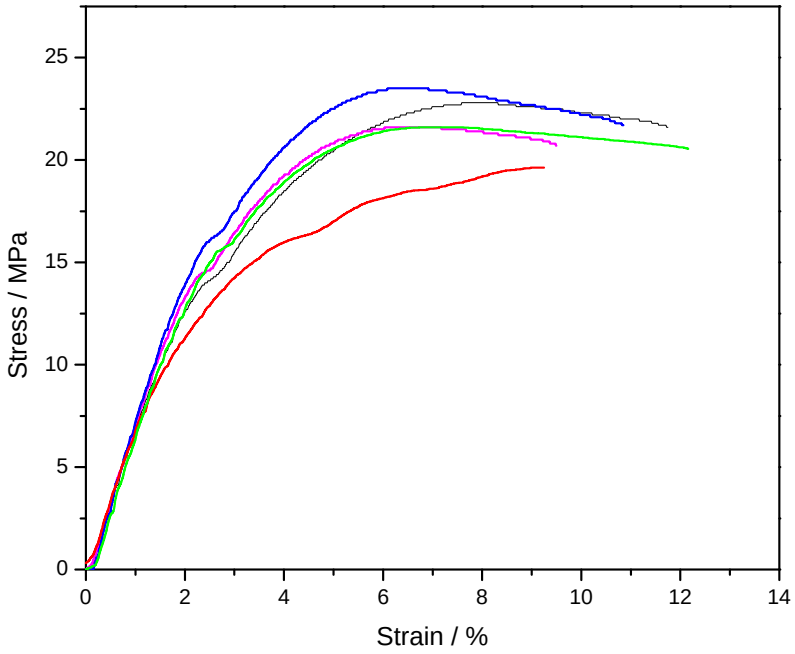

Figure A.2 Stress-strain curves of 80/20 w/w PP/(PS:wax)

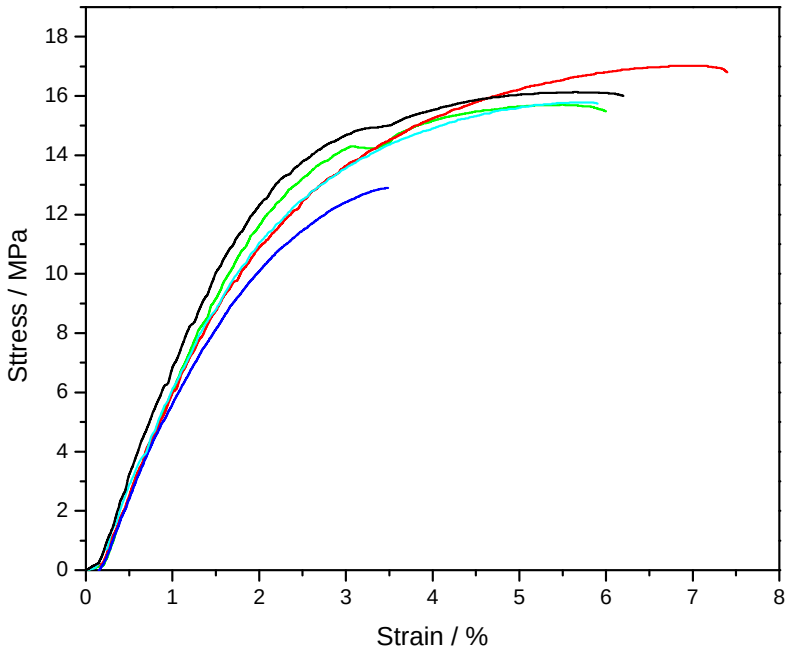

Figure A.3 Stress-strain curves of 70/30 w/w PP/(PS:wax)

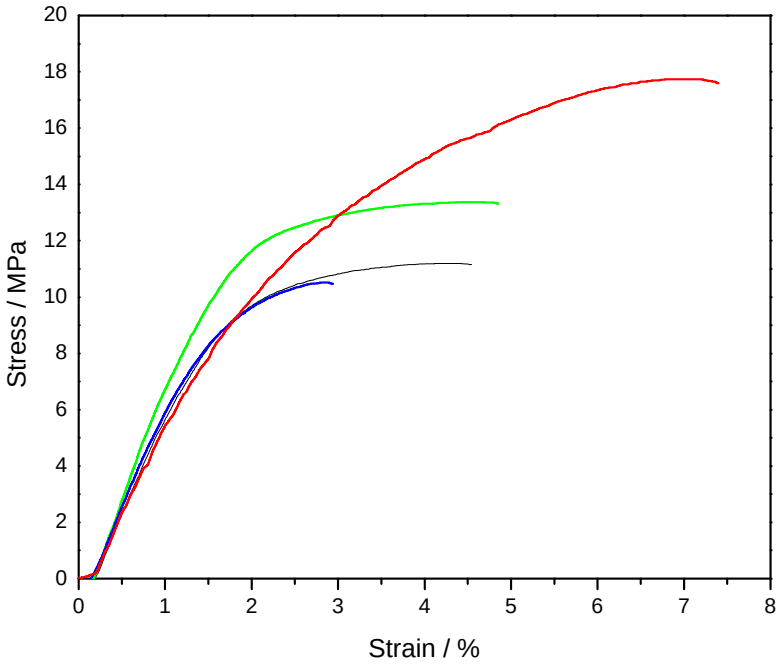

Figure A.4 Stress-strain curves of 60/40 w/w PP/(PS:wax)

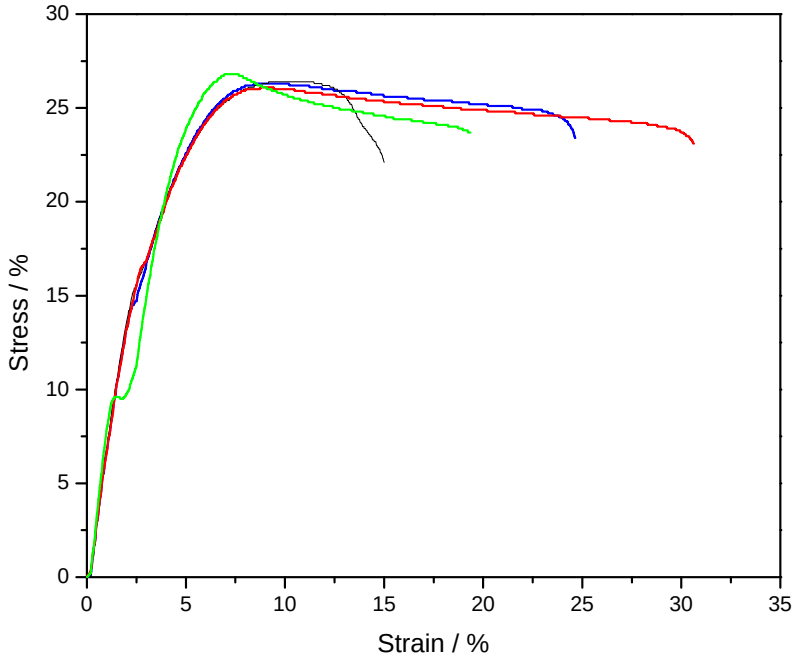

Figure A.5 Stress-strain curves of 82.5/10/7.5 w/w PP/(PS:wax)/SEBS

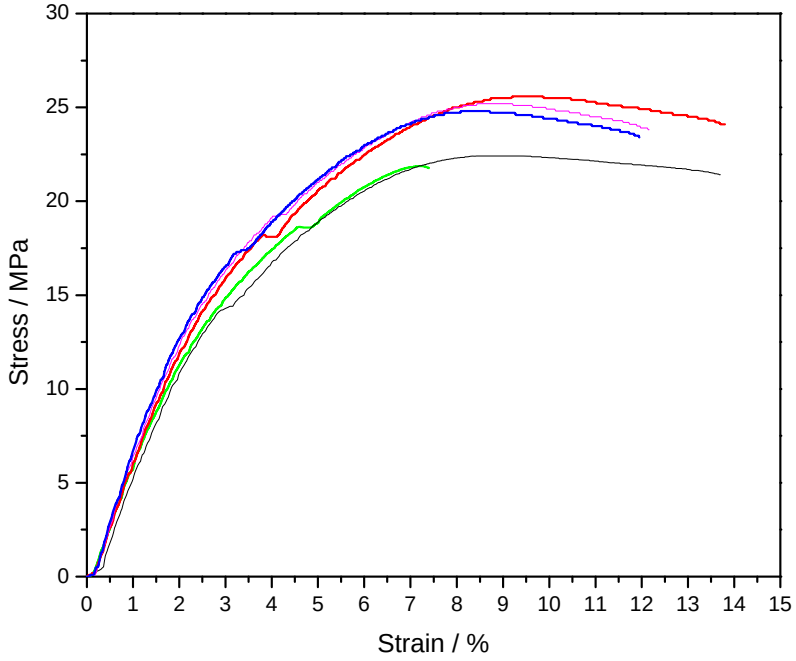

Figure A.6 Stress-strain curves of 72.5/30/7.5 w/w PP/(PS:wax)/SEBS

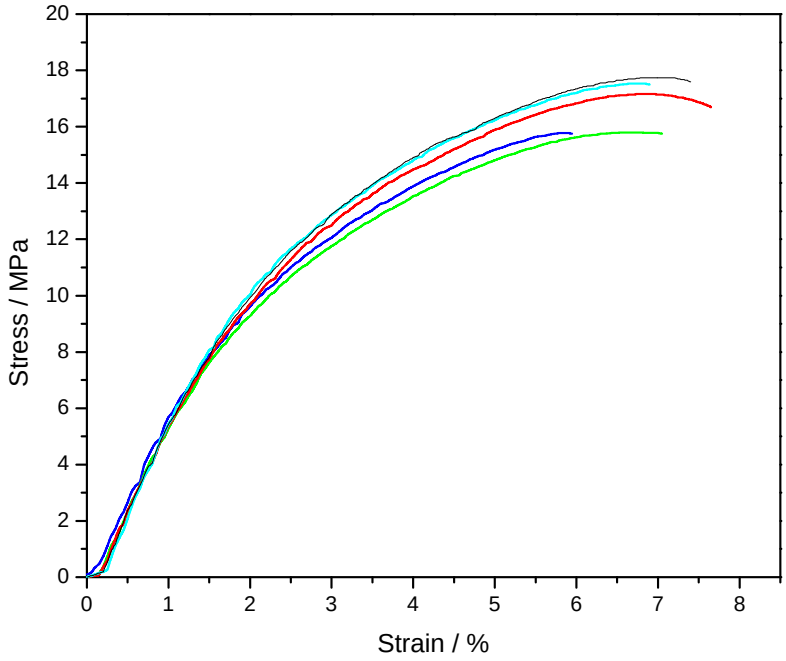

Figure A.7 Stress-strain curves of 52.5/40/7.5 w/w PP/(PS:wax)/SEBS

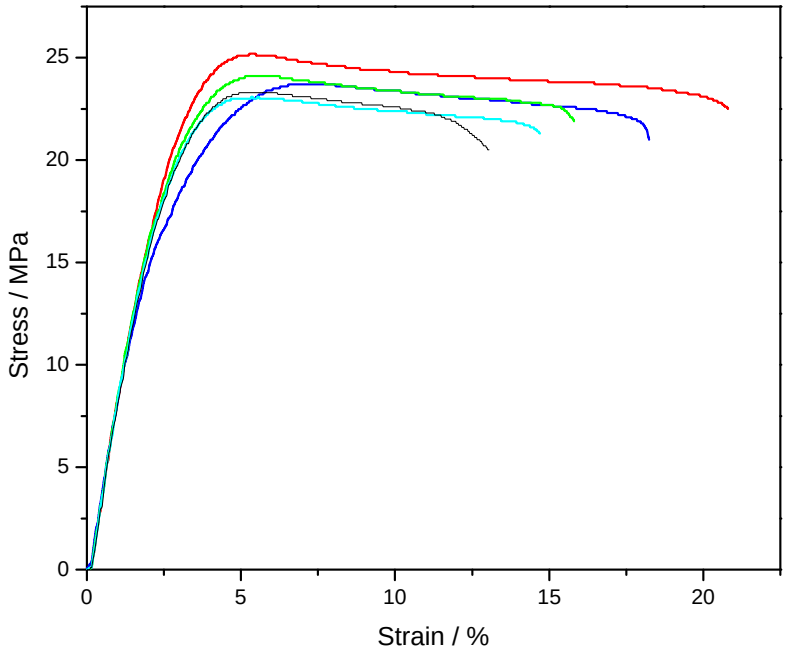

Figure A.8 Stress-strain curves of 90/10 w/w PP/PS

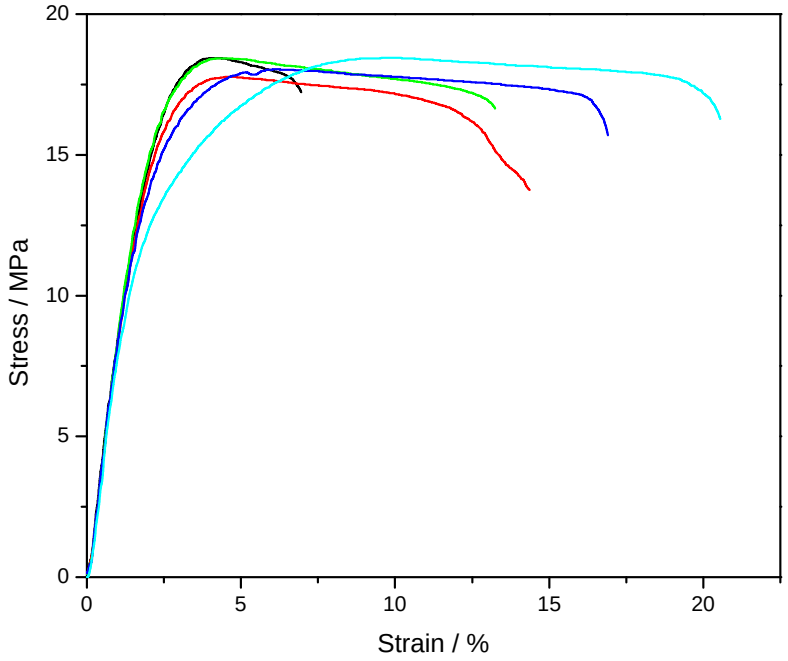

Figure A.9 Stress-strain curves of 70/30 w/w PP/P

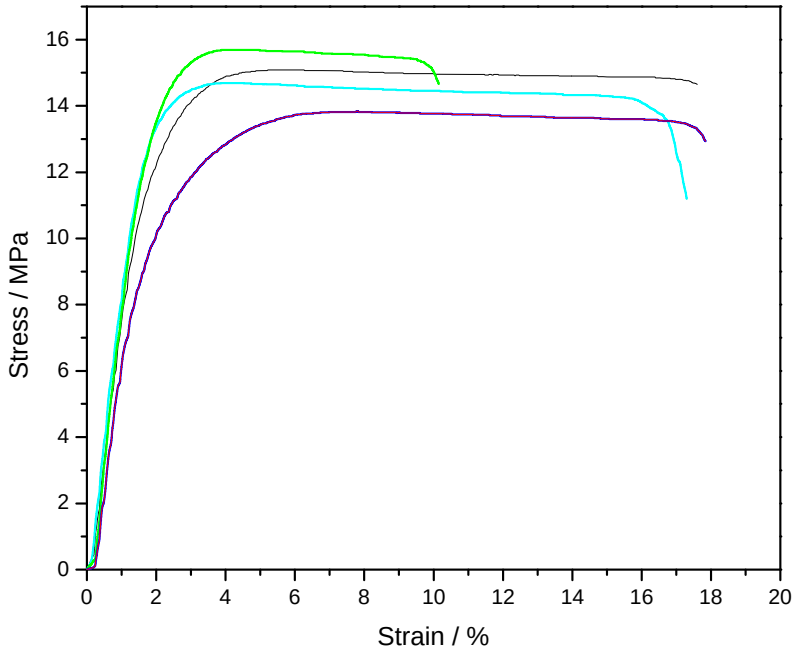

Figure A.10 Stress-strain curves of 60/40 w/w PP/PS

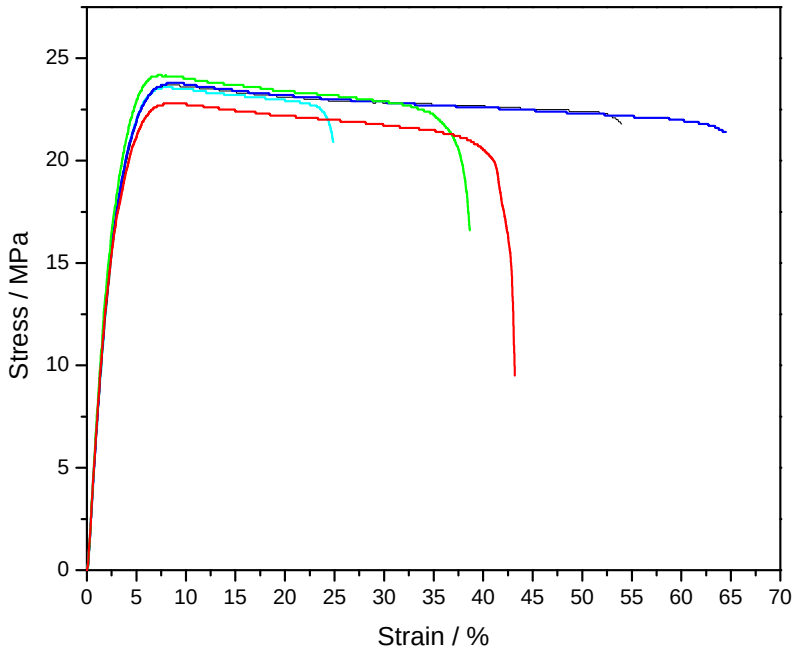

Figure A.11 Stress-strain curves of 82.5/10/7.5 w/w PP/PS/SEBS

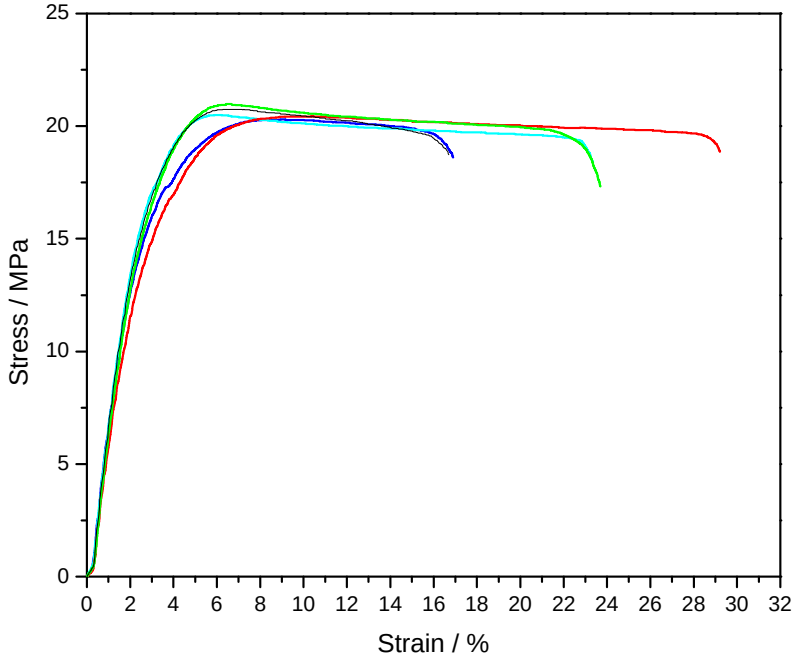

Figure A.12 Stress-strain curves of 72.5/20/7.5 w/w PP/PS/SEBS

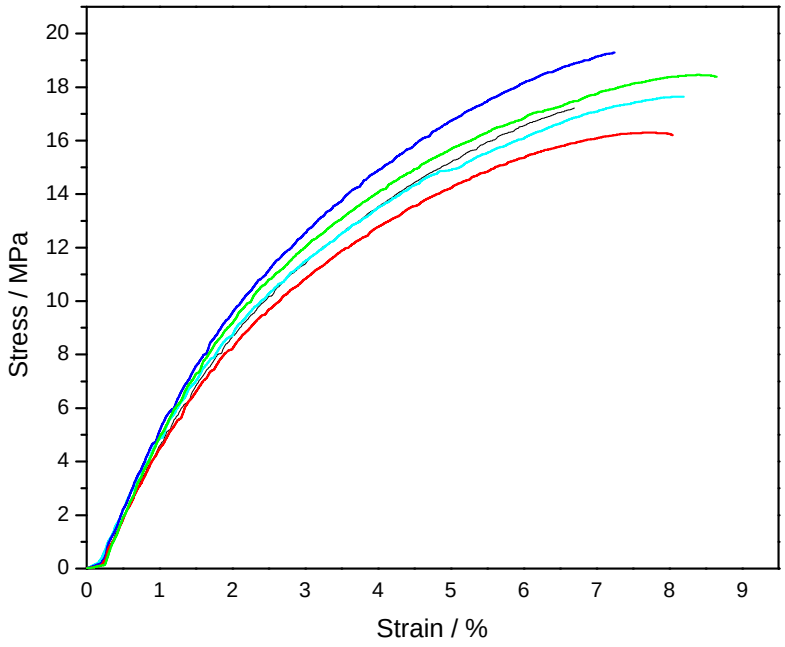

Figure A.13 Stress-strain curves of 62.5/30/7.5 w/w PP/PS/SEBS